Modeling and Design of Vapor-Phase Biofiltration for Chlorinated Volatile Organic Compounds

Walter Den and Massoud Pirbazari
Dept. of Civil and Environmental Engineering, University of Southern California, Los Angeles, CA 90089

A mathematical model was developed for biofilter design and performance prediction with reference to the purification of contaminated gas streams. The model incorporated important aspects such as mass transfer, biodegradation, and adsorption processes. A systematic modeling protocol incorporated the development of a scale-up strategy based on dimensional analysis and similitude. Trichloroethylene (TCE) was employed as the model contaminant for biofiltration testing and model verification. The biokinetic and adsorption parameters for the contaminant were determined independently from a series of minibiofilter and miniadsorber column experiments, specifically designed to simulate the actual biofilter operational regimes in a miniature scale. Bench-scale biofilter experiments employing granular activated carbon columns indicated the good predictive capability of the model for the removal of TCE. Dynamic simulation studies were performed to assess the transient- and steady-state behavior of the model under various operating conditions. Model sensitivity was studied to evaluate the influence of adsorption equilibrium, transport and biological parameters on the biofilter dynamics. The results demonstrated that the biofilter performance was greatly influenced by the Monod coefficients and the biofilm thickness.

Introduction

Industrial gas-phase emissions of hazardous contaminants including volatile organic compounds (VOCs) are widely regarded as risks to environmental and occupational health. A broad spectrum of innovative treatment technologies are currently available for the control of such industrial emissions, among which biofiltration is a viable alternative. The biofiltration process involves the growth of heterotrophic microorganisms immobilized on a solid surface and sustained by the organic components of the gas stream. The technology has several advantages over traditional physical or chemical processes such as thermal destruction, carbon adsorption, and liquid scrubbing; and these include low energy consumption, and, consequently, low operating and maintenance costs. Furthermore, granular activated carbon (GAC) employed as a biofilter packing material not only provides a favorable environment for biofilm growth, but also extends the contact time between the biofilm and contaminants due to its desirable adsorptive characteristics. These beneficial features attributed to the adsorptive characteristics of GAC and biodegradative ability of the biofilm are particularly important in the degradation of recalcitrant compounds. These aspects have been well addressed by several researchers in both aqueous-phase systems (Ying and Weber, 1979; Kim and Pirbazari, 1989; Ravindran et al., 1997) and in gas-phase systems (De heyder et al., 1994; Man et al., 1996).

An important aspect regarding implementation of full-scale biofiltration systems is their economic planning and design. A modeling and design protocol may indeed be a valuable tool to minimize the scope of elaborate, time-consuming, and expensive pilot-scale testing normally considered before a full-scale design is contemplated upon. Therefore, the present study focuses on the development of a mathematical modeling technique for performance prediction and simulation of biofilters under various operating conditions. The proposed model has the versatility of using either adsorbing or nonadsorbing media. The study is also intended to establish a systematic approach in determining the model input parameters, and to verify the predictive capability of the model. In the present study, GAC was employed as the biofilter pack-

Correspondence concerning this article should be addressed to M. Pirbazari.
Current address of W. Den: Dept. of Environmental Science, Tunghai University, Tai-Chung, Taiwan.

ing medium, and trichloroethylene (TCE) was chosen as the model compound.

Background

Rationale for the choice of TCE as test compound

TCE ranks among the most extensively used chlorinated solvents in a variety of industries, including electronics, metal finishing/degreasing, and painting operations, and is a VOC of importance from an air-pollution control perspective. It is highly volatile due to its high vapor pressure (58 mm Hg at 25°C and 1 atm) and Henry's Law constant (1×10^{-2} atm-m^3/mol), and, therefore, evaporates rapidly from the aqueous phase. Additionally, TCE is listed among 189 hazardous air pollutants (HAPs) in Section 112 of the 1990 Clean Air Act amendment (CAAA, 1990). It is recognized by the U.S. Environmental Protection Agency (EPA) as a suspected human carcinogen, capable of causing damage to the central nervous system on exposure at high concentrations (Miller and Guengerich, 1983). Furthermore, TCE represents a spectrum of recalcitrant chlorinated compounds, and provides a more rigorous *modus operandi* for testing the performance of biofiltration technology, and evaluating the predictive capability of the biofilter model.

Review on Previous Biofiltration Models

In recent years, several gas-phase biofiltration models have been proposed. The earliest model developed by Diks and Ottengraf (1991) considered a two-phase mass-transfer process between gaseous phase and biofilm for treatment of dichloromethane using a ceramic packing material. It further assumed that mass transfer in the gaseous phase was predominantly controlled by biofilm diffusion, and that biofilm degradation followed zero-order kinetics. This model laid the fundamental framework for biofiltration modeling, although it was limited to steady-state conditions. Shareefdeen and Baltzis (1994) extended the model conceptualization of Ottengraf and coworkers by introducing a mass-transfer term between the gaseous and solid phases to represent sorption effects. These researchers employed a mixture of peat and perlite as biofilter packing media. They also considered oxygen limitation by incorporating companion mass balance equations for oxygen consumption, and employed the Andrews-Haldane inhibitory kinetics for describing the biodegradation of methanol, benzene, and toluene. Subsequently, Hodge and Devinny (1995) employed a two-phase mass-transfer concept to characterize the transport mechanisms in a biofilter using ethanol as the model compound and compost, GAC, or a mixture of compost and diatomaceous earth as packing media. Their model assumed first-order kinetics to describe the biodegradation of ethanol (an easily biodegradable VOC). They also estimated carbon dioxide evolution rates to support the first-order biokinetics hypothesis by assuming a stoichiometric relationship between ethanol mineralization and carbon dioxide production. Deshusses et al. (1995) developed a model to describe both steady-state and transient-state dynamics of a biofilter, packed with a mixture of compost and polystyrene spheres, for treatment of methyl ethyl ketone (MEK) and methyl isobutyl ketone (MIBK). Their model treated the solid surface as an extension of biofilm. The models discussed above showed a good predictive capability for their respective model compounds. However, they were limited to nonadsorbing media due to the absence of terms describing adsorption dynamics.

More recently, Wang and Govind (1997) developed a steady-state model to predict biofilter performance for treating isopentane using a bed packed with peat and compost. They assumed that biodegradation occurred within the particle, and described the biokinetics by a "double Monod" expression to include both substrate concentration and water contained in the particle. Their model also established the effects of water content on biofilter performance. More recently, Sun et al. (1998) developed an axial dispersion-convection model for biofiltration of TCE using a pure strain of bacteria. Their model incorporated cometabolic biodegradation and focused on the effects of deactivation of the TCE-degrading enzyme and the transformation capacity of active biomass.

The present model, like its predecessors, addresses all important phenomena occurring in a biofilter including biofilm diffusion, biodegradation, adsorption, and axial gas transport. The model, however, incorporates certain additional features to describe substrate transport, including the following: (i) film transport through the external liquid layer, and (ii) intraparticle diffusion inside the adsorbent phase. It should be noted that the incorporation of these features into the model would expand its applicability to various types of porous granular media including soils and zeolites.

Biofiltration Modeling for Performance Forecasting

Model conceptualization and assumptions

The conceptualization of the biofilter model is graphically depicted in Figure 1. The model considers a spherical adsorbent particle, a biofilm of constant thickness, an external liquid film with defined thickness, and a hydrodynamic gas layer. As a result, contaminants undergo consecutive phase transfer processes from gas to liquid, followed by diffusion and biodegradation within the biofilm, and eventually adsorption onto the solid surface. Since each layer (gas film, water layer, and biofilm) surrounding the spherical particle is assumed to be of uniform thickness, these layers also form a spherical configuration on the exterior of the particle surface. The effect of curvature is fully accounted for by applying the one-dimensional (1-D) (that is, radial coordinate) diffusion equation for each spherical layer. Biodegradation is described by the classical Monod kinetics, and oxygen transport through the biofilm is not considered to be a rate-limiting factor. Moreover, the particles are assumed to be uniform in size, with adsorption sites evenly distributed throughout the particle volume. Two equilibrium relationships are included as boundary conditions coupling the contaminant concentrations at heterogeneous phases: Henry's Law between gaseous- and liquid-phase concentrations, and the Freundlich isotherm between the liquid- and solid-phase concentrations. Additional assumptions pertaining to the model are described below:

(1) No bulk gas concentration gradient occurs axially within any incremental bed layer. This implies that each individual

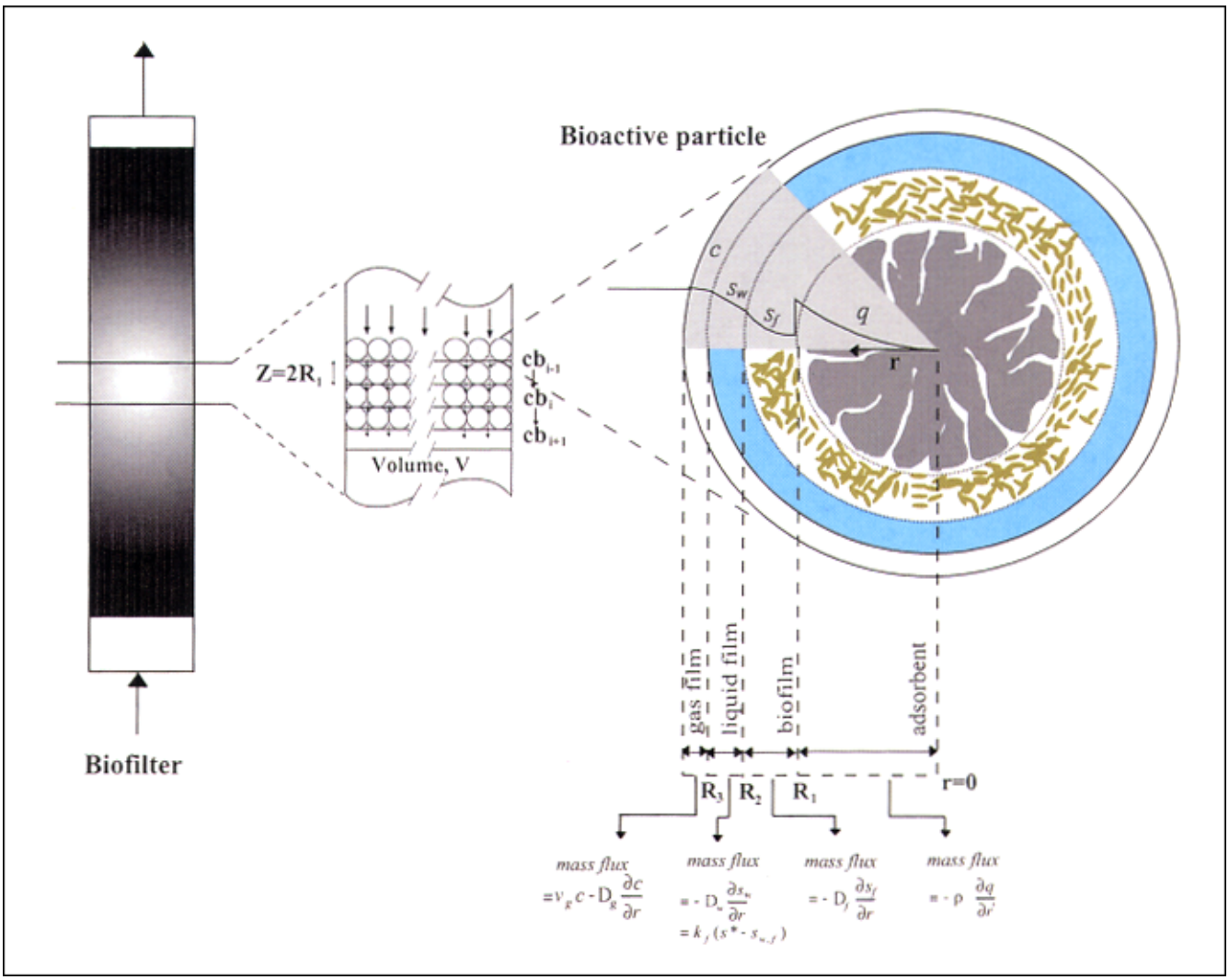

Figure 1. Biofilter model conceptualization.

particle in the axial increment experiences identical conditions (advection, dispersion, and concentration) to proceed with the subsequent transport and reaction, and, hence, no interaction occurs between adjacent particles.

(2) The biofilm formed is idealized as a homogeneous, stagnant layer with uniform thickness and cell density surrounding the exterior of the particle surface.

(3) Biodegradation occurs strictly within the biofilm domain, an assumption that has two important implications. Firstly, the primary role of the external liquid layer surrounding the biofilm is to present a mass-transfer resistance barrier caused by the moisturization of the biofilter bed. Secondly, as the substrate reaches the adsorbent surface, adsorption is considered the only operative mechanism.

(4) Adsorption is a reversible process driven by concentration gradients, and its equilibrium is characterized by the Freudlich isotherm.

(5) Substrate migration along the pore walls, referred to as "surface diffusion," is the dominant mechanism, and that diffusion through the pores is considered insignificant. Therefore, the mass transport in the adsorbent particle is characterized by a surface diffusion coefficient.

Model Formulations

Based on the preceding assumptions, the mass balance equations for the organic contaminant in each domain are formulated in the ensuing sections.

Hydrodynamic gas film

Assuming a constant gas flow velocity, the mass balance for the hydrodynamic gas film is depicted by the advection-diffusion equation

$$\frac{\partial c}{\partial t} + v_g \frac{\partial c}{\partial r} = D_g \frac{1}{r^2} \frac{\partial}{\partial r}\left[r^2 \frac{\partial c}{\partial r} \right] \tag{1}$$

where v_g is the constant gas velocity, and D_g is the substrate diffusion coefficient in air. The terms in Eq. 1, from left to right, represent the rate of change of pollutant concentration in the gas phase, the rate of net pollutant transport by advection, and the rate of diffusion transport into the adsorbent volume. The initial and boundary conditions are

$$c(r, t = 0) = 0 \tag{1a}$$

$$D_g \frac{\partial c(r=R_3,t)}{\partial r} = k_f(s^* - s_{w,f}) \tag{1b}$$

$$c(r \to \infty, t) = c_b \tag{1c}$$

where k_f is the mean mass-transfer coefficient across the water film, s^* represents the substrate concentration at the gas-water interface, $s_{w,f}$ represents the substrate concentration at the water-biofilm interface, and c_b denotes the substrate concentration in the bulk gas. The first boundary condition (Eq. 1b) states that the mass flux into and out of the gas-water interface must be equivalent. The second boundary condition states that the substrate concentration beyond the gas film is virtually equal to the concentration in the bulk gas phase, since the gas-film thickness is considered negligible compared to the distance in the pore space between particles.

External liquid phase

The water layer surrounding the biofilm due to the media over-moisturization causes additional mass-transfer resistance to substrate molecules (Speitel and McLay, 1993; Wang and Govind, 1997). Applying the following equation includes this aspect

$$\frac{\partial s_w}{\partial t} = D_w \frac{1}{r^2} \frac{\partial}{\partial r}\left[r^2 \frac{\partial s_w}{\partial r}\right] \tag{2}$$

where D_w is the substrate diffusion coefficient in water. The initial and boundary conditions are the following

$$s_w(r,t=0) = 0 \tag{2a}$$

$$D_w \frac{\partial s_w(r=R_2,t)}{\partial r} = D_f \frac{\partial s_f(r=R_2,t)}{\partial r} \tag{2b}$$

$$s_w(r=R_3,t) = \frac{c(r=R_3,t)}{H_c} \tag{2c}$$

The boundary condition (Eq. 2b) establishes the equivalence between the mass fluxes into and from the water-biofilm interface. The boundary condition (Eq. 2c) represents the Henry's Law constant, relating the substrate concentrations in gaseous and liquid phases.

Biofilm

Mass transport within the biofilm is described by a diffusion equation similar to that applied to the adsorbent phase. The reaction term in this particular domain is characterized by the classic Monod biodegradation kinetics. The equation combining mass transport and biodegradation can therefore be written as follows

$$\frac{\partial s_f}{\partial t} = D_f \frac{1}{r^2} \frac{\partial}{\partial r}\left[r^2 \frac{\partial s_f}{\partial r}\right] - X_f \frac{\mu_m s_f}{K_s + s_f} \tag{3}$$

where D_f is the substrate diffusion coefficient in the biofilm, X_f is the constant biomass density, and μ_m and K_s are the Monod constants.

The appropriate initial and boundary conditions are

$$s_f(r,t=0) = 0 \tag{3a}$$

$$D_f \frac{\partial s_f(r=R_1,t)}{\partial r} = D_s \rho_s \frac{\partial q(r=R_1,t)}{\partial r} \tag{3b}$$

$$s_f(r=R_2,t) = s_w(r=R_2,t) \tag{3c}$$

The first boundary condition (Eq. 3b) establishes that the mass flux into the solid/biofilm interface must be equivalent to that leaving the interface. The second boundary condition describes the continuity of the substrate mass flux at the water-biofilm interface.

Adsorbent phase

The substrate undergoes phase transfer at the particle surface after penetrating the biofilm. The adsorbed substrate is subsequently transported to the inner pore-wall of the particle, driven by the concentration gradient along the particle radius. The transport is diffusion into the adsorbent particle and is described by the classic 1-D diffusion equation governed by an intraparticle diffusion coefficient D_s, written as shown below in spherical coordinates as

$$\frac{\partial q}{\partial t} = \frac{D_s}{r^2} \frac{\partial}{\partial r}\left[r^2 \frac{\partial q}{\partial r}\right] \tag{4}$$

with an initial condition

$$q(r,t=0) = 0 \tag{4a}$$

and two boundary conditions

$$\frac{dq(r=0,t)}{dr} = 0 \tag{4b}$$

$$q_s = q(r=R_1,t) = K_f s_{f,s}^{\,n} \tag{4c}$$

The concept underlaying the diffusive transport of the contaminant into the adsorbent particle is well discussed in earlier publications by Crittenden and Weber (1978a,b). The first boundary condition describes a symmetric concentration profile over the entire particle, with no concentration gradient at its center. The second boundary condition is the Freundlich isotherm, relating the solid-phase concentration at the biofilm-solid interface, where K_F and n represent the Freundlich isotherm constants.

Substrate molecules accumulate within as they penetrate deeper into the adsorbent particle. Upon reaching its ultimate adsorption capacity, the adsorbent will be "saturated" and will discontinue substrate uptake. In this regard, the accumulated or adsorbed quantity of contaminants (substrates) per particle can be computed from the following equations

$$dM = qdV_p \tag{5}$$

and

$$M = \int_0^{R_1} qdV_p = 4\pi \int_0^{R_1} qr^2 dr \tag{5a}$$

Bulk gas phase

The axial transport of the bulk gas is graphically illustrated in Figure 1. As previously stated in assumption 1, the substrate mass removed from the bulk gas within each bed layer must be equal to the mass lost to each particle times the number of particles in the layer. This concept may be described in mathematical terms by

$$c_{b,i+1} = \frac{M_{in,i} - \Delta M_{\text{total},i}}{V_L} \tag{6}$$

where

$$M_{in,i} = c_{b,i} \times V_L \tag{6a}$$

and

$$\Delta M_{\text{total},i} = N_p \Delta M_i = N_p \left[\int_{R_2}^{R_3} s_w(r) dV_p + \int_{R_1}^{R_2} s_f(r) dV_p + \int_0^{R_1} q(r) dV_p \right] \tag{6b}$$

In the above equations, $M_{in,i}$ and $\Delta M_{\text{total},i}$ represent the substrate input mass and the total mass removed in the axial layer designated as i, respectively, $c_{b,i+1}$ denotes the substrate concentration in the next layer designated as $i+1$, ΔM_i is the newly accumulated mass in a single particle, V_L is the volume of the bed layer, and N_p is the number of particles in an axial layer.

Numerical Solution

Dimensional analysis and similitude techniques have proven useful for process design and scale-up. The following dimensionless variables are then defined for mathematical expediency to establish meaningful dimensionless parameters

$$\bar{c} = \frac{c}{C_{in}};\ \bar{s}_f = \frac{s_f}{s_0};\ \bar{s}_w = \frac{s_w}{s_0};\ \bar{q} = \frac{q}{q_0};\ \bar{r} = \frac{r}{R_1};\ \tau = \frac{tv_g}{L};$$

$$s_0 = \frac{C_{in}}{H_c};\ q_0 = K_F (s_0)^n \tag{7}$$

Substituting these dimensionless variables into the governing equations (Eqs. 1–6), the following dimensionless groups can be defined

$$\alpha_s = \frac{D_s L}{R_1^2 v_g};\ \alpha_f = \frac{D_f L}{R_1^2 v_g} = \frac{St}{Sh};\ \alpha_w = \frac{D_w L}{R_1^2 v_g};\ \alpha_g = \frac{D_g L}{R_1^2 v_g};$$

$$\delta = \frac{L}{R_1};\ \phi_1 = \left(\frac{D_s}{D_f}\right)\left(\frac{\rho_s q_0}{s_0}\right) = \left(\frac{D_s}{D_f}\right) D_{g,s};\ \phi_2 = \left(\frac{D_f}{D_w}\right);$$

$$\omega_1 = \frac{X_f \mu_m R_1}{v_g s_0};\ \omega_2 = \frac{K_s}{s_0};\quad \gamma = \frac{k_f R_1}{D_g H_c} = \frac{St\, Pe}{\delta^2 H_c} \tag{8}$$

where

$$St = \text{Stanton number} = \frac{k_f L}{v_g R_1} \tag{9}$$

$$Sh = \text{Sherwood number} = \frac{k_f R_1}{D_f}; \tag{10}$$

$$Pe = \text{column Peclet number} = \frac{L v_g}{D_g} \tag{11}$$

and

$$D_{g,s} = \text{surface solute distribution parameter} = \left(\frac{\rho_s q_0}{s_0}\right) \tag{12}$$

Furthermore, the two dimensionless groups involving biological and adsorption kinetics, namely the biochemical reactivity modulus (E_r) and the surface diffusivity modulus (E_s), can be formulated as follows

$$E_r = \frac{D_f Da_{ov} \tau_c}{R_1^2} \tag{13}$$

$$E_s = \frac{D_s D_{g,s} \tau_c}{R_1^2} \tag{14}$$

where

$$\tau_c = \frac{L}{v_g} \tag{15}$$

and

$$\frac{1}{Da_{ov}} = \frac{1}{Da_s} + \frac{1}{Da_{ft}} \tag{16}$$

The significance of the above dimensionless groups must be briefly reviewed in view of their immense importance from a process scaling perspective for biofilters. The Stanton number represents the ratio between liquid film transport and bulk transport of the contaminant. The Sherwood number denotes the ratio between liquid film transport and biofilm diffusive transport. The Peclet number is the ratio between bulk transport and gas-phase diffusive transport, while the

surface solute distribution parameter is a measure of the contaminant distribution between the adsorbent surface and the gas phase. The biochemical reactivity modulus represents the ratio of the biochemical reaction rate to the overall transport rate for the contaminant, while the surface diffusivity modulus signifies the ratio of surface diffusivity (into the adsorbent) to the bulk transport of the contaminant.

In Eq. 16, Da_s, Da_{ft}, and Da_{ov} represent the Damköhler numbers pertaining to surface diffusivity, film transfer, and overall mass transport, respectively. These dimensionless groups can be defined as follows

$$Da_{ft} = \frac{k^* R_1}{k_f} \tag{17}$$

and

$$Da_s = \frac{k^* R_1^2}{D_s} \tag{18}$$

where

$$k^* = \frac{X_f \mu_m}{K_s} \tag{19}$$

The Damköhler numbers generally denote the ratio of the reaction rate to the transport rate of the contaminant, and each specific Damköhler number represents the ratio of the rate of biochemical reaction to the rate of the corresponding transport mechanism.

The system of equations to be solved assume the following forms after substitution of the dimensionless parameters listed in Eq. 8 (the equations were numbered in accordance to their respective original form of equations)

Hydrodynamic Gas Film

$$\frac{\partial \bar{c}}{\partial \tau} + \delta \frac{\partial \bar{c}}{\partial \bar{r}} = \alpha_g \frac{1}{\bar{r}^2} \frac{\partial}{\partial \bar{r}} \left[\bar{r}^2 \frac{\partial \bar{c}}{\partial \bar{r}} \right] \tag{20}$$

$$\bar{c}(\bar{r}, \tau = 0) = 0 \tag{20a}$$

$$\frac{\partial \bar{c}\left(\bar{r} = 1 + (R_2 + R_3)/R_1, \tau\right)}{\partial \bar{r}} = \gamma\left(\bar{s}^* - \bar{s}_{f,s}\right) \tag{20b}$$

$$\bar{c}(\bar{r} \to R_4/R_1, \tau) = 1 \tag{20c}$$

External Liquid Phase

$$\frac{\partial \bar{s}_w}{\partial \tau} = \alpha_w \frac{1}{\bar{r}^2} \frac{\partial}{\partial \bar{r}} \left[\bar{r}^2 \frac{\partial \bar{s}_w}{\partial \bar{r}} \right] \tag{21}$$

$$\bar{s}_w(\bar{r}, \tau = 0) = 0 \tag{21a}$$

$$\frac{\partial \bar{s}_w\left(\bar{r} = 1 + (R_2/R_1), \tau\right)}{\partial \bar{r}} = \phi_2 \frac{\partial \bar{s}_f\left(\bar{r} = 1 + (R_2/R_1), \tau\right)}{\partial \bar{r}} \tag{21b}$$

$$\bar{s}_w\left(\bar{r} = 1 + (R_2 + R_3)/R_1, \tau\right) = \bar{c}\left(\bar{r} = 1 + (R_2 + R_3)/R_1, \tau\right) \tag{21c}$$

Biofilm

$$\frac{\partial \bar{s}_f}{\partial \tau} = \alpha_f \frac{1}{\bar{r}^2} \frac{\partial}{\partial \bar{r}} \left[\bar{r}^2 \frac{\partial \bar{s}_f}{\partial \bar{r}} \right] - \frac{\omega_1 \bar{s}_f}{\omega_2 + \bar{s}_f} \tag{22}$$

$$\bar{s}_f(\bar{r}, \tau = 0) = 0 \tag{22a}$$

$$\frac{\partial \bar{s}_f(\bar{r} = 1, \tau)}{\partial \bar{r}} = \phi_1 \frac{\partial \bar{q}(\bar{r} = 1, \tau)}{\partial \bar{r}} \tag{22b}$$

$$\bar{s}_f\left(\bar{r} = 1 + \frac{R_2}{R_1}, \tau\right) = \bar{s}_w\left(\bar{r} = 1 + \frac{R_2}{R_1}, \tau\right) \tag{22c}$$

Adsorbent Phase

$$\frac{\partial \bar{q}}{\partial \tau} = \alpha_s \frac{1}{\bar{r}} \frac{\partial}{\partial \bar{r}} \left[\bar{r}^2 \frac{\partial \bar{q}}{\partial \bar{r}} \right] \tag{23}$$

$$\bar{q}(\bar{r}, \tau = 0) = 0 \tag{23a}$$

$$\frac{d\bar{q}(\bar{r} = 0, \tau)}{d\bar{r}} = 0 \tag{23b}$$

$$\bar{q}(\bar{r} = 1, \tau) = \bar{q}_s = \bar{s}_{f,s}{}^n \tag{23c}$$

Bulk Gas

$$c_{b,i+1} = \frac{\overline{M}_{\text{in},i} - \Delta \overline{M}_{\text{total},i}}{V_L} \tag{24a}$$

$$\Delta \overline{M}_{\text{total},i} = N_p \Delta \overline{M}_i = N_p \times \left[\int_{R_2/R_1}^{R_3/R_2} \bar{s}_w(\bar{r}) d\overline{V}_p + \int^{R_2/R_1} \bar{s}_f(\bar{r}) d\overline{V}_p + \int_0^1 \bar{q}(\bar{r}) d\overline{V}_p \right] \tag{24b}$$

The model essentially consists of a set of coupled partial differential equations (PDEs) with a 2-D (r,t) system, which is solved by adopting an implicit finite difference scheme. In this scheme, all differential operators are first discretized into a system of ordinary differential equations (ODEs) by applying the backward difference formula with time derivatives. The system of ODEs is then solved iteratively until the difference between two consecutive solutions satisfies the prescribed tolerance limit for convergence. Although this iterative method requires more computational steps, it has the advantage of avoiding the problem of manipulating large matrices under stiff concentration gradients. Once the mass flux transported into the particles is obtained by solving the system of PDEs, the axial mass transport (expressed in discrete form without time variation in the model formulation) can be computed by directly subtracting the total mass flux lost into the particles from the incoming mass flux.

Dimensional Analysis, Similitude, and Scale-Up Considerations

Process upscaling can be accomplished by dimensional analysis and similitude techniques. Dimensional analysis is a powerful tool for dealing with complex physical, chemical, and biological systems, and can describe the phenomenological

aspects of scaling in relatively simple relationships (Blöschl and Sivapalan, 1995). Its utilities can be briefly summarized as follows: (a) it defines similarity in relationships among dimensionless groups without reference to individual parameters; (b) it establishes relationships valid over a wide range of scales; (c) it serves as a powerful tool for data reduction; and (d) it characterizes the dominant mechanisms in the process. The concept of similitude refers to the similarity between two systems from a geometric, phenomenological, or dynamic standpoint, so that characteristics of one system can be related to those of others by a conversion factor. Similarity analysis is more powerful than dimensional analysis because it can handle more than one unit, and can also handle dimensionless quantities (Blöschl and Sivapalan, 1995). In this regard, a deterministic mathematical model proves useful in identifying important physical and chemical/biological subprocesses in biofiltration for developing appropriate scaling criteria. Such an approach used for upscaling processes would greatly reduce costs and time associated with the design of pilot- and full-scale systems.

In biofiltration processes employing microporous adsorbent particles as packing media, the kinetics of film transfer, biodegradation, and adsorption must be considered for developing scale-up criteria. The dimensionless parameters previously described (Eqs. 8–19) suggest that biofiltration can be characterized by the following nondimensional groups: the Peclet number (Pe), the Stanton number (St), the Damköhler number (Da), the surface diffusivity modulus (E_s), and the biochemical reactivity modulus (E_r). It should be noted that the Monod biokinetic constants (μ_m and K_s) are considered intrinsic properties of microbial cultures, and are independent of geometric and dynamic properties. The solute distribution parameter ($D_{g,s}$) also remains unchanged for a certain contaminant and biofilter medium. These conditions require identical values in the following properties: (i) influent concentration; (ii) particle density and packing porosity; (iii) Monod kinetic constants; and (iv) Freundlich isotherm parameters.

Assuming that the biofilter model provides excellent predictions for small-scale biofilters, a good *a priori* performance evaluation and design for large-scale biofilters can be obtained by comparing the seven dimensionless groups identified above. Setting the values of some of them equal for small-scale and large-scale biofilters, certain scaling relationships among major design variables were established. The important design and operation parameters for scaling relate to the following aspects: (1) particle size; (2) reactor dimensions; (3) adsorption kinetics; and (4) biodegradation kinetics. The scaling equations can be formulated on two possible assumptions regarding particle size and adsorption kinetics—the surface diffusion coefficient is independent of the particle size, or is a linear function of particle size. The scaling criteria developed here address both cases. Additionally, the relationship between particle size and biodegradation kinetics is established by comparisons of the reactivity modulus and overall Damköhler numbers corresponding to small-scale and large-scale biofilters. It is indeed the case that all seven dimensionless groups cannot be held constant for scaling because one of them would control the ultimate design. Nevertheless, certain minimum or maximum values of dimensionless groups must be maintained to accomplish a feasible, practical, and near-optimal design. As the large-scale process is usually designed based on experimental results obtained from the small-scale version, a major consideration would be the incorporation of saftey criteria to guarantee the desired performance levels in large-scale systems. In order to meet this objective, the following equality or inequality criteria must be satisfied

$$St_L > St_S, \quad Pe_L < Pe_S, \quad E_{s,L} > E_{s,S}, \quad E_{r,L} > E_{r,S}, \quad (25)$$

and

$$Da_{ov,L} = Da_{ov,S}$$

In all scaling equations, the subscripts "S" and "L" represent the small-scale and large-scale systems, respectively. The Stanton number criterion will ensure that the large-scale biofilter does not undergo channeling without adequate film transfer. The Peclet number criterion may not be significant in a gas-phase biofilter where axial dispersion effects are negligible. The adsorption modulus criterion assures that the large-scale reactor has sufficient adsorbent capacity to withstand shock loading, while the biochemical reactivity modulus criterion insures that there is sufficient biodegradation in the large-scale reactor to accomplish the desired level of contaminant degradation.

The important scaling variables are biofilter dimensions (length and diameter), packing medium particle sizes, and empty bed contact time (EBCT). In order to account for the concomitant processes (mass transfer, biofilm degradation and adsorption) in the upscaling operation, three different scenarios must be considered. Evaluation of Da_{ov} leads to the following scale-up scenarios:

Case I. Biodegradation is the predominant mechanism ($Da_{ov} \approx Da_{ft}$ and $Da_{ov} \gg 1$): Such cases represent biofiltration of pollutants with very low surface diffusivity (nonadsorbent or nonadsorbing chemical). Therefore, the removal process is biokinetically rate limiting.

Case II. Adsorption is the predominant mechanism ($Da_{ov} \approx Da_s$ and $Da_s \ll 1$): Such cases describe biofiltration of highly adsorbable and slowly biodegradable compounds. Therefore, adsorption is the primary removal mechanism.

Case III. Both biodegradation and adsorption are significant mechanisms: In such cases, an intermediate factor must be determined to account for both processes.

The scale-up relationship for Case I can be developed by equating the biochemical reactivity modulus E_r

$$\frac{EBCT_L}{EBCT_S} = \frac{\tau_{c,L}}{\tau_{c,S}} = \left(\frac{R_{1,L}}{R_{1,S}}\right)^2 \left(\frac{Da_{ov,S}}{Da_{ov,L}}\right) \quad (26)$$

where $EBCT_L$ and $EBCT_S$ represent the EBCTs corresponding to large- and small-scale systems, respectively. If the Damköhler number is held constant for upscaling, then the EBCT is proportional to the square of the particle size. However, variation in the particle sizes may also reflect on the values of Da_{ov}, since the film transfer rate (k_f) and the biofilm density (X_f) could sometimes be dependent on particle sizes.

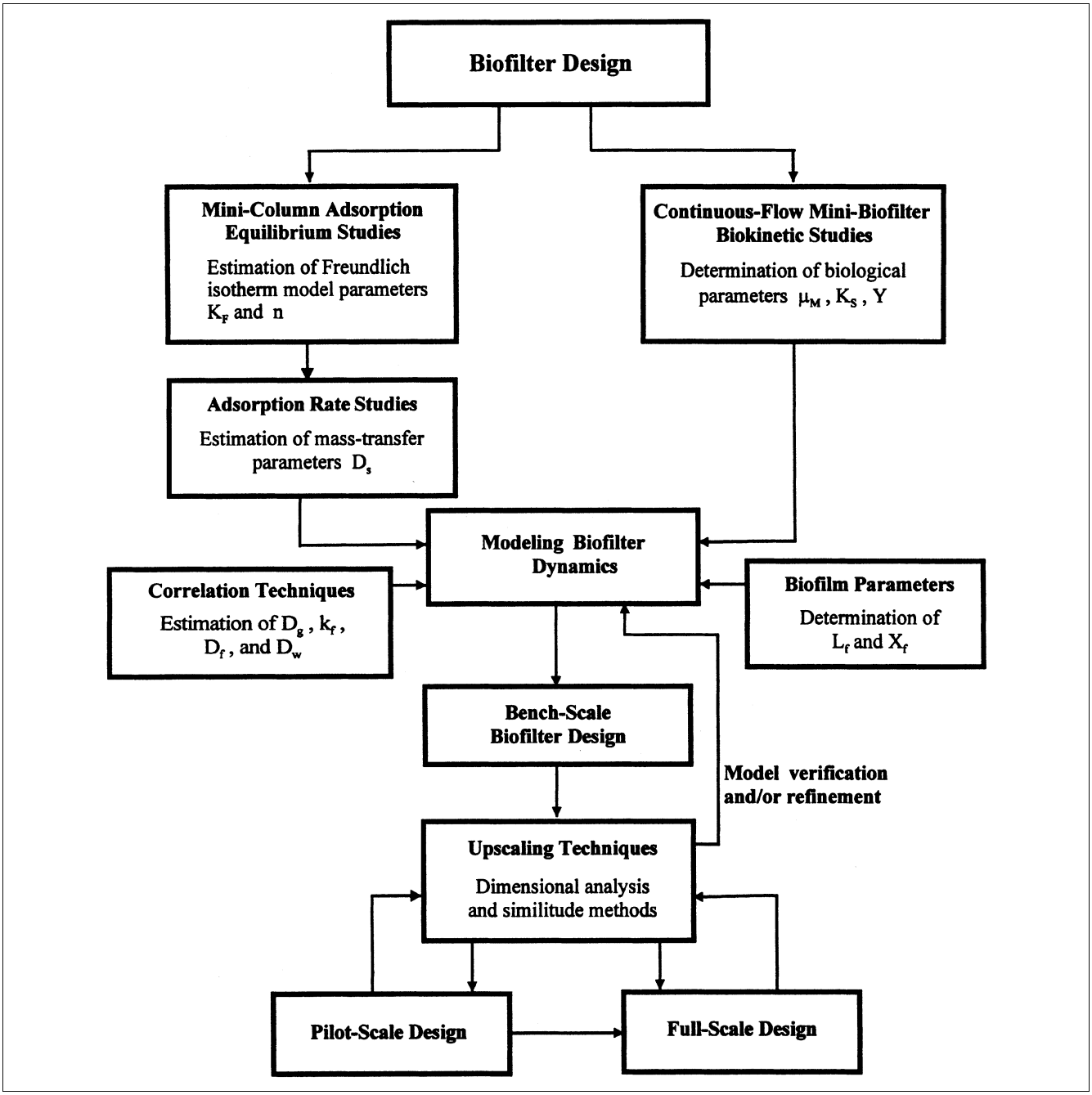

Figure 2. Protocol for modeling, design and scale-up of biofilters.

Case II essentially represents an adsorber, whose scale-up methods have been previously developed by Crittenden and coworkers (Crittenden and Hand, 1986; Crittenden et al., 1987) and subsequently employed by Pirbazari and coworkers (1991, 1993). If the intraparticle mass transfer is controlled by surface diffusivity, then the scale-up relationship can be written as

$$\frac{EBCT_L}{EBCT_S} = \frac{\tau_{c,L}}{\tau_{c,S}} = \left(\frac{R_{1,L}}{R_{1,S}}\right)^2 \left(\frac{D_{s,S}}{D_{s,L}}\right)^{\alpha} \tag{27}$$

where α defines the power of dependence of the surface diffusivity on particle size, and $\tau_{c,L}/\tau_{c,S}$ is the ratio of breakthrough time for the large- and small-scale systems. For example, when the constant surface diffusivity condition ($\alpha = 0$, independent of the particle size) is assumed, the scale-up relationship becomes

$$\frac{EBCT_L}{EBCT_S} = \frac{\tau_{c,L}}{\tau_{c,S}} = \left(\frac{R_{1,L}}{R_{1,S}}\right)^2 \tag{28}$$

On the other hand, when the surface diffusivity is assumed proportional to the particle size ($\alpha = 1$), then the scale-up relationship takes the form

$$\frac{EBCT_L}{EBCT_S} = \frac{\tau_{c,L}}{\tau_{c,S}} = \left(\frac{R_{1,L}}{R_{1,S}}\right) \tag{29}$$

Case III, which represents a scenario where both biofilm degradation and adsorption contribute significantly to the overall removal process, should exhibit an intermediate scale-up relationship between Cases I and II. A weighted residual technique can be applied to Eqs. 26 and 27 by introducing a factor β to encompass the relative importance of biodegradation or adsorption. Therefore, a generalized scale-up relationship can be expressed as

$$\frac{EBCT_L}{EBCT_S} = \frac{\tau_{c,L}}{\tau_{c,S}} = \left[\left(\frac{R_{1,L}}{R_{2,S}}\right)^2\left(\frac{Da_S}{Da_L}\right)\right]^{\beta}\left[\left(\frac{R_{1,L}}{R_{1,S}}\right)^2\left(\frac{D_{s,S}}{D_{s,L}}\right)^{\alpha}\right]^{1-\beta}$$

$$= \left(\frac{R_{1,L}}{R_{1,S}}\right)^2\left(\frac{Da_{ov,S}}{Da_{ov,L}}\right)^{\beta}\left(\frac{D_{s,S}}{D_{s,L}}\right)^{\alpha(1-\beta)} \qquad 0 \le \beta \le 1 \tag{30}$$

The value of β can be superimposed on the value of Da_{ov} when the reaction kinetics and surface diffusion coefficient are known, but must be determined empirically for greater accuracy. However, if the overall Damköhler number and surface diffusivity are both independent of the particle sizes, then Eq. 28 must be used as the scale-up relationship.

General Protocol for Biofilter Modeling and Design

A design approach essentially consists of a mathematical model capable of describing various phenomenological interactions associated with the process. The model is primarily employed to forecast the operational dynamics of biofiltration systems, and to evaluate the effects of various operational variables on their performance. A modeling and design protocol, such as that outlined in Figure 2, can be an effective tool for pilot- and full-scale biofilter design. The procedure also involves a series of rigorous experimental techniques to evaluate the important model parameters governing its predictive capability. Mini-column GAC adsorber experiments are conducted to evaluate the adsorption equilibrium parameters for the target contaminant(s). The adsorption equilibrium parameters are used in conjunction with parameter-search techniques to estimate the mass-transfer coefficient governing adsorption kinetics, as described in an earlier article (Ravindran et al., 1999). Concurrently, biokinetic and biofilm parameters are obtained from a series of continuous-flow, mini-biofilter experiments using nonadsorbing packing media. It should be noted that these mini-biofilter studies provide an improvement over conventional methods for determination of biological parameters by closely simulating the dynamics and operating regimes of real biofilters. Conventional methods generally involve batch culture studies such as the suspended shake-flask experiments, where the biokinetic parameters are estimated from changes in biomass and contaminant concentrations over time. Subsequently, a series of bench-scale biofilter experiments are designed based on the "feedforward" approach provided by the model with the adsorption and biological parameters. The results from bench-scale experiments, in turn, provide the necessary feedback to validate the model's predictive capability, and to implement model refinements if needed.

Subsequent to model verification, scale-up strategies are developed employing dimensional analyses and similitude as previously discussed. The scale-up method is an integral part of the protocol leading to *a priori* evaluation of pilot- and full-scale designs from laboratory-scale results. This approach of combining experimental procedures and modeling techniques serves as an efficient and cost-effective method for design of full-scale biofilter systems, whereby pilot-scale testing can be treated as a confirmatory rather than an exploratory procedure. Under this scenario, only limited pilot-scale biofilter testing would be required before implementing full-scale operations. However, it must be noted that the subsequent steps outlined in the protocol involving pilot- and full-scale design are beyond the scope of this study. The applicability of the protocol could be extended to biofilters with nonadsorbing media, such as ceramics, plastics, polymers, and other synthetic materials, wherein adsorption studies are omitted.

Materials and Methodologies

Materials

Packing Materials.

Nonadsorbing medium. SIRAN carriers (Schott Glaswerke, Mainz, Germany), which are silicated, open-pore sintered glass beads, serve as nonadsorbing packing media for the continuous-flow biokinetic studies. These spherical carriers are specifically designed for immobilization of microorganisms during clinical and biotechnological processes. The SIRAN carriers have a particle size range of 1 to 2 mm, an average macropore diameter of 120 μm, and a surface area of 87 m^2/L (0.15 m^2/g).

Adsorbing medium. Bituminous-based BPL vapor-phase GAC (Calgon Corporation, Pittsburgh, PA) was used as the adsorbing packing medium for biofilter column experiments. The selected GAC has a standard mesh size of 4×6, and surface area of 950–1,100 m^2/g. In order to minimize channeling and wall effect in miniadsorber columns, the granular carbon was grinded and sieved. Carbon particles with mesh size of 35×40 were collected, washed, and oven dried at 105°C before sealing in a screw-cap container until usage.

Synthetic Waste Air.

TCE vapor. The TCE used in this study was of A.C.S. grade and was obtained from Fisher Scientific (Fairlawn, NJ). A modification of the diffusion cell apparatus described by McKelvey and Hoelscher (1957) was used for continuous-flow TCE vapor generation at low concentrations (< 10 ppm). An additional impinger was installed in the diffusion cell to generate higher TCE concentration. The diffusion cell was completely immersed in heated water bath regulated by a temperature controller (Model TE-8D, Techne, Cambridge, U.K.) to vaporize the solvent. The vapor diffusing through the dif-

fusion tube was mixed with the air stream prior to entering the biofilter column.

Microorganisms.

The microbial cultures were obtained by acclimating mixed liquor taken from a wastewater treatment plant in a chemostat reactor (Kontes Glass, Vineland, NJ). Glucose was added to the suspension during the initial phase of acclimation, but was gradually replaced by TCE as the only carbon source. The packing medium was seeded with a mixed consortium consisting of at least four strains of bacteria, as observed by applying the serial isolation technique. Inorganic nutrients were routinely supplied for the growth of microorganisms in

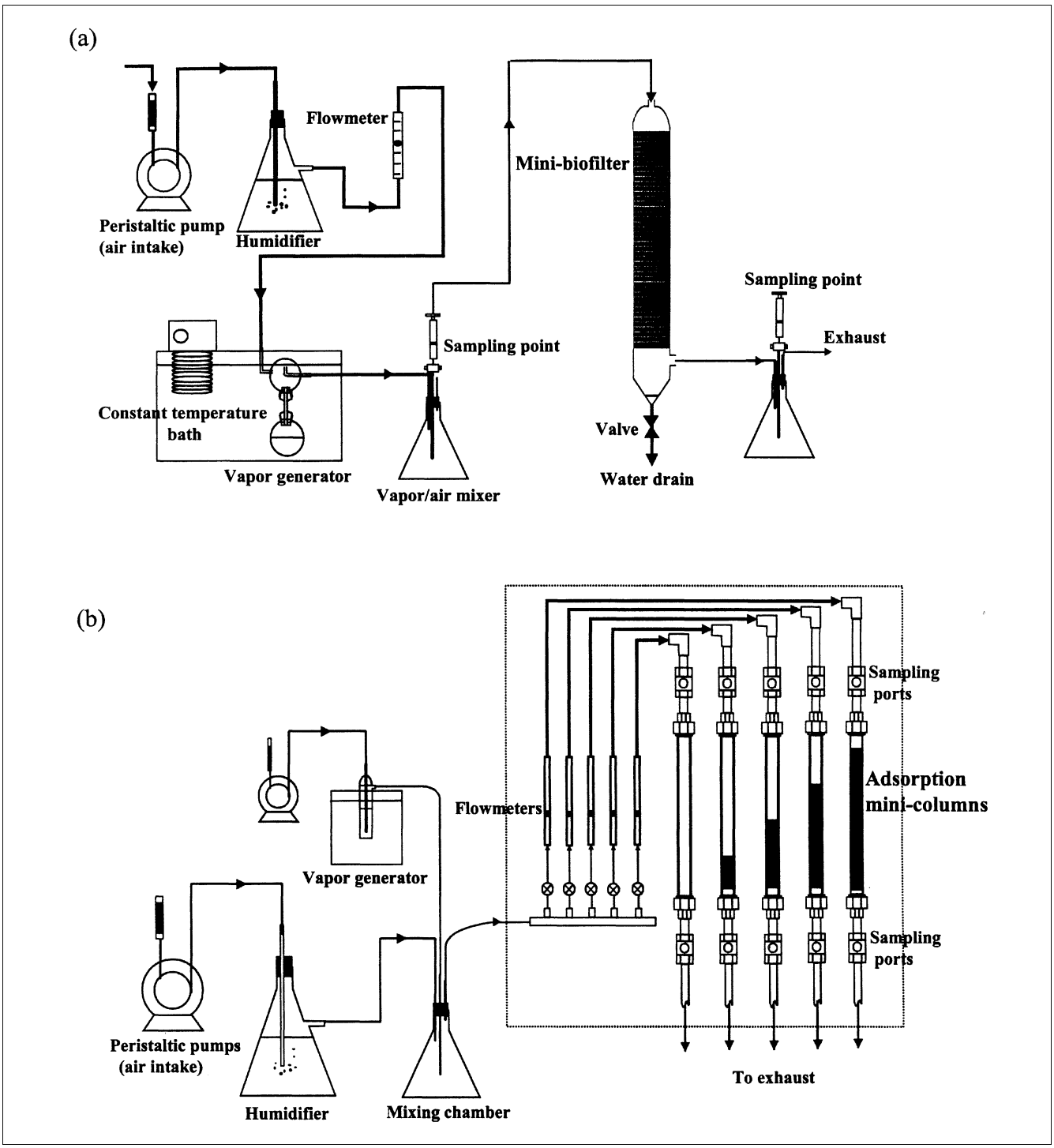

Figure 3. (a) Minibiofilter experimental setup for biokinetic studies; (b) miniadsorber column experimental setup for isotherm determination.

biofilters. The nutrient composition is listed as follows: KH_2PO_4, 85 mg/L; K_2HPO_4, 217.5 mg/L; $NaNO_3$, 120 mg/L; NH_4Cl, 25 mg/L; $MgSO_4 \cdot 7H_2O$, 22.5 mg/L; $CaCl_2$, 27.5 mg/L; $FeCl_3 \cdot 6H_2O$, 0.25 mg/L; $MnSO_4 \cdot H_2O$, 0.0399 mg/L; H_3BO_3, 0.0572 mg/L; $ZnNO_3 \cdot 7H_2O$, 0.0428 mg/L; $(NH_4)_6Mo_7O_2$, 0.0347 mg/L; $FeCl_3 \cdot$ EDTA, 0.1 mg/L. Trace quantities of growth enhancers were also added to the inorganic nutrient to accelerate the growth of microorganisms in the biofilter. The growth enhancers included the following components: biotin, 6 μg/L; riboflavin, 15 μg/L; nicotinic acid, 15 μg/L; B_{12}, 0.3 μg/L; thioctic acid, 15 μg/L; folic acid, 6 μg/L; thiamin, 15 μg/L; pantothenic acid, 15 μg/L; p-aminobenzoic acid, 15 μg/L.

Analytical techniques

TCE Analysis. Biofilter influent and effluent TCE vapor concentrations were measured by a gas chromatograph (Perkin Elmer Sigma 2B, Norwalk, CT) equipped with a flame ionization detector and interfaced with an integrator (Spectra Physics, Santa Clara, CA). A 6-ft glass column packed with 0.1% SP-1000 on 80/100 CarboPak C (Supelco, Bellefonte, PA) was used as the chromatographic column. Helium was employed as the carrier gas at a flow rate of 30 mL/min, whereas hydrogen and oxygen were used as combustion gases at flow rates of 30 mL/min and 28 mL/min, respectively. Carbon disulfide (CS_2) was used as carrier solvent to prepare solution standards for TCE. The gas chromatograph was operated isothermally at a temperature of 130°C, while the injector and detector were maintained at temperatures of 200°C and 300°C, respectively.

Carbon Dioxide Measurement. A titrimetric technique modified from the biometer method developed by Bartha and Pramer (1965) was adopted for the quantitative analysis of carbon dioxide at low concentrations in mini-biofilter experiments. Approximately 20 to 25 mL of 0.1N potassium hydroxide (KOH) were used as a scrubbing solution to effectively dissolve gaseous CO_2. Approximately 10 milliliters of sample were then withdrawn for titration with 0.1N HCl. Prior to titration, 1 milliliter of 2N $BaCl_2$ was added to the sample to precipitate out H_2CO_3 in the form of $BaCO_3$.

Methodologies

Biokinetic studies. Continuous-flow minibiofilter (internal diameter, 2.5 cm; packing depth, 45 cm) experiments were designed, as shown in Figure 3, to provide an accurate and realistic approach for estimating biokinetic parameters. The biofilters were packed with SIRAN particles as a nonadsorbing medium to simulate TCE removal solely attributed to biodegradation phenomenon. The medium was seeded with an acclimated culture prior to packing into the mini-biofilters. Various influent concentrations and gas flow rates were investigated. The column operation for each set of influent concentration or flow rate was continued for at least 30 days until steady-state removal was observed. Duplicate samples withdrawn from the sampling ports at the inlet and outlet ends of the biofilters were analyzed on a regular basis. Biomass measurements were performed at the end of each biofilter experiment by the gravimetric method (Tang and Fan, 1987; Tang et al., 1996). Approximately equal amounts of samples were carefully taken from the top, middle, and bottom portion of the biofilter column. The samples (original weight W_0) were then oven-dried at 105°C for at least 10 h to completely evaporate water (W_1), followed by combustion at 550°C for 30 min to burn off the carbon residuals. Finally, the samples were washed with weak nitric acid (HNO_3) to remove particle residuals, and oven-dried again at 105°C (W_2). The weight difference between W_0 and W_1 represented the wet biomass used to compute the biofilm thickness, whereas the difference between W_0 and W_2 was used to estimate the biofilm dry density.

Adsorption studies. Adsorption equilibrium parameters were determined from a series of minicolumn adsorption experiments in a manner similar to that discussed by Kim and Pirbazari (1989) for aqueous systems. These experiments were specifically designed to estimate the adsorption parameters independent of biological and dispersion effects. The minicolumn system is shown in Figure 3. Influent gas streams mixed with various concentrations of TCE were introduced into an adsorption manifold comprising five minicolumns (including a control column) in parallel packed with different quantities of GAC. With the same operating conditions, namely, the influent concentration, flow rate, temperature, and so on, the breakthrough profile for each column was determined by periodic analysis of samples from effluent streams. The gas streams were conditioned with water vapor to simulate the actual operating conditions in a biofilter (relative humidity > 85%). Adsorption parameters including the sorption capacity and intensity constants, as well as the surface diffusion coefficient, were estimated from the breakthrough profiles.

Bench-Scale Biofilter Column Studies. Three bench-scale biofilter experiments were designed and operated to evaluate the TCE removals in realistic reactor systems, and validate the predictive capability of the model. The biofilter columns

Table 1. Operating Characteristics of Bench-Scale Biofilters for Model Verification

Exp. Desig.	Fig. No.	Microbial Inoculum	Avg. Influent Conc. (ppmv)	Avg. Flow Rate (L/min)	EBCT (min)
BF-1	6	Mixed culture 1*	20	0.45	4.5
BF-2	7	Mixed culture 1*	20	1.0	2.0
BF-3	8	Mixed culture 2†	15	2.0	1.0

*Biokinetic parameters were determined in this study.
†Biokinetic parameters were not determined in this study.
All experiments were conducted using columns with internal diameter of 7 cm and length of 60 cm.

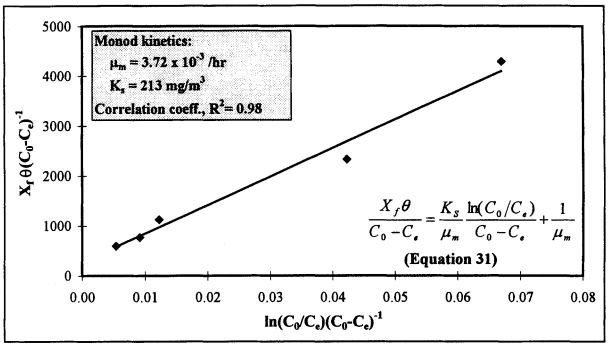

Figure 4. Experimental minibiofilter data and Monod kinetic model for TCE.

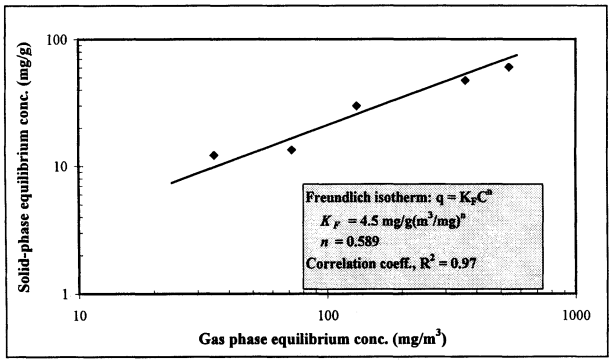

Figure 5. Experimental minicolumn adsorption equilibrium data and Freundlich isotherm model for TCE.

were of identical size (i.d., 7 cm; height, 60 cm), and were packed with appropriate quantities of GAC. Two of the biofilters were inoculated with the same TCE-degrading cultures, with the third biofilter seeded with a different microbial consortium. These columns were subjected to various operating conditions as specified in Table 1.

Results and Discussion

Determination of model parameters

Biological Parameters. Biological parameters including biokinetic constants, carbon dioxide evolution rates, and biofilm thickness and density were determined from the mini-biofilter experiments. The biokinetic parameters including the Monod half-saturation constant (K_S) and maximum substrate utilization rate (μ_m) were estimated by using the linearized version of mass balance equations for a plug-flow reactor under steady-state conditions

$$\frac{X_f\theta}{C_0 - C_e} = \frac{K_s}{\mu_m}\frac{\ln\,(C_0/C_e)}{C_0 - C_e} + \frac{1}{\mu_m} \qquad (31)$$

Figure 4 shows a plot of $X_f\theta/(C_0 - C_e)$ and $\ln(C_0/C_e)/(C_0 - C_e)$ with good linear correlation, from which K_s and μ_m were estimated as 213 mg/m^3 and 3.7×10^{-3} hr^{-1}, respectively. The microbial yield coefficient Y was estimated as 0.15 based on CO_2 evolution measurement.

The biofilm density (X_f) and biofilm thickness (L_f) were estimated from biomass measurements conducted after each biokinetic experiment using appropriate empirical correlations (Law et al., 1976; Pirbazari et al., 1993)

$$\text{Biofilm Thickness:}\quad L_f = \frac{\Delta W_1}{\rho_l N_p A_p(0.99)} \qquad (32)$$

$$\text{Dry Biomass Density:}\quad X_f = \frac{\Delta W_2}{N_p A_p L_f} \qquad (33)$$

The average values for biofilm thickness ($L_f \approx 21\ \mu$m) and biomass density ($X_f \approx 2{,}800$ g/m^3) were used as the biokinetic parameters of choice.

Adsorption Equilibrium Parameters. The mini-column adsorption experiments facilitated the generation of a series of TCE breakthrough profiles corresponding to different influent concentrations and GAC masses. The Freudlich isotherm was found to provide the most appropriate representation of equilibrium data. Figure 5 shows the linearized plot of adsorption capacities vs. influent concentrations employing the logarithmic version of the Freudlich relation

$$\text{Log}_{10}(q) = \log_{10}(K_F) + n\,\log_{10}(C_0) \qquad (34)$$

The values of the Freundlich isotherm constants, K_F and n, were determined to be 4.5 mg/g (m^3/mg)^n and 0.59, respectively.

Mass-Transfer Parameters. The mass transfer parameters include the intraparticle surface diffusion coefficient (D_s), the external film transfer coefficient (k_f), as well as substrate diffusion coefficient in air (D_x), in liquid film (D_w), and in biofilm (D_f).

The intraparticle surface diffusion coefficient was independently estimated by adopting the parameter-search technique involving the homogeneous surface diffusion model (HSDM) (Crittenden and Weber, 1978a,b; Crittenden et al., 1987, 1991; Kim and Pirbazari, 1989; Pirbazari et al., 1993). The parameter D_s, which represents the diffusion of the compound along the pore-wall surfaces, determines the uptake rate of a compound by activated carbon, and its value was validated by simulating the mini-column adsorption breakthrough profiles using the nonbioactive version of the biofiltration model (Ravindran et al., 1999).

The substrate diffusion coefficient in air can be estimated from the correlation method proposed by Fuller et al. (1966) based on molecular diffusivity

$$D_g = \frac{0.0010T^{1.75}\sqrt{\dfrac{1}{M_1} + \dfrac{1}{M_2}}}{P\left[(\Sigma v)_1^{1/3} + (\Sigma v)_2^{1/3}\right]^2} \qquad (35)$$

where ν_I represents the molar volume, M is the molar mass, and the subscripts 1 and 2 correspond to TCE vapor and air

molecules, respectively. The constants T and P denote the absolute temperature (K) and pressure (atm), respectively.

The liquid diffusion coefficient D_w can be estimated from empirical correlations for dilute liquid mixtures. A detailed review on this aspect is presented by Taylor and Krishna (1993), comparing the estimates of diffusion coefficients obtained from different correlations for polar and nonpolar binary mixtures composed of nonelectrolytes at dilute concentrations. The different correlations employed for estimating the free liquid diffusivities of organic compounds in aqueous solutions are as follows

Wilke and Chang (1955)

$$D_w = 7.4\times10^{-8}\frac{(\psi_b M_b)^{0.5}T}{\mu_b \nu_a^{0.6}} \tag{36}$$

Hayduk and Laudie (1974)

$$D_w = 13.26\times10^{-5}\mu_b^{-1.14}V_a^{-0.589} \tag{36a}$$

Hayduk and Minhas (1983)

$$D_w = 1.25\times10^{-8}\left(V_a^{-0.19}-0.292\right)\mu_b^{(9.58/V_a-0.292)}V_a^{-0.589}T^{1.52} \tag{36b}$$

Siddiqi and Lucas (1986)

$$D_w = 2.98\times10^{-7}\mu_b^{-1.026}V_a^{-0.589}T \tag{36c}$$

In the above correlations ν_a represents the molar volume of the organic compound (TCE), and ψ_b, μ_b, M_b denote the association parameter, absolute viscosity, and molar mass of water, respectively. T denotes the absolute temperature. In this study, the choice of the Wilke and Chang correlation was rationalized on the basis of the following observations. Taylor and Krishna (1993) evaluated the suitability of the above correlations for several organic compounds in aqueous systems including methanol, propanol, and several VOCs. They observed that the Wilke and Chang (1955) correlation generally provided the best estimates for most aqueous systems at low temperatures, while the Hayduk and Laudie (1974) method gave good estimates over the entire temperature range. They further noted that the Hayduk and Minhas (1983) estimates were not as accurate, but still good for engineering purposes; whereas, the Siddiqi and Lucas (1986) approach consistently underpredicted the diffusivities. It is interesting to note that the variability in the diffusion coefficients for TCE estimated by different correlations was within the range of 5–10% from the Wilke and Chang values.

Diffusion of contaminants in biofilm is generally slower than that in water due to the additional resistance attributed to dense microorganisms and their extracellular secretions. In general, the higher the density of the biofilm, the lower is the substrate diffusivity. Fan et al. (1990) proposed an empirical equation to correlate the substrate diffusion coefficient in biofilm and water based on the biofilm density (X_f)

$$\frac{D_f}{D_w} = 1-\frac{0.43X_f^{0.92}}{11.19+0.27X_f^{0.99}} \tag{37}$$

The external film transfer coefficient for a packed bed of spherical particles can be evaluated using the empirical correlation proposed by Dwivedi and Upadhyay (1977)

$$Sh = \left(0.765Re_p^{0.18}+0.365Re_p^{0.614}\right)\frac{Sc^{1/3}}{\epsilon} \tag{38}$$

The dimensionless groups in the above correlation, namely the Sherwood (Sh), Reynolds (Re_p), and Schmidt (Sc) num-

Table 2. Values of Model Parameters for Typical Biofilter Model Simulations

Parameter	Notation	Description	Unit	Value
Mass-transfer parameters	D_s	Substrate diffusivity in solid	m^2/h	7.5×10^{-9}
	D_f	Substrate diffusivity in biofilm	m^2/h	3.1×10^{-6}
	D_w	Substrate diffusivity in water layer	m^2/h	3.4×10^{-6}
	D_g	Substrate diffusivity in gas film	m^2/h	3.2×10^{-2}
	k_f	Substrate film transfer rate through water-biofilm	m/h	2.1×10^{-3}
Physicochemical parameters	K_F	Freundlich isotherm constant	$(mg/g)(m^3/mg)^n$	4.5
	n	Freundlich isotherm constant	—	0.59
	R_1	Particle radius	m	2.0×10^{-3}
	L_w	Water layer thickness	m	20×10^{-6}
	L_a	Arbitrary distance in gas stream away from particle surface	m	5.0×10^{-4}
	H_c	Gas-liquid equilibrium (Henry's Law) constant	—	0.40
	N_p	Number of particle in a layer	—	245
	ρ_s	Particles packing density	g/m^3	4.5×10^5
Biological parameters	μ_m	Maximum substrate utilization rate	L/h	3.72×10^{-3}
	K_s	Half-saturation constant	g/m^3	0.213
	Y	Microbial yield coefficient	mg/mg	0.15
	L_f	Biofilm thickness	m	21×10^{-6}
	X_f	Biofilm density	g/m^3	2.82×10^3

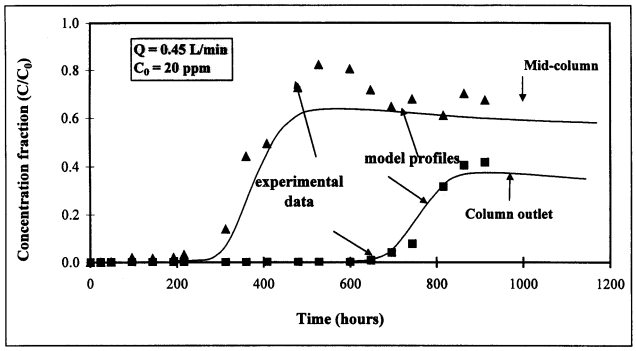

Figure 6. Experimental data and model profiles for TCE in BF-1 at mid-column and column outlet positions.

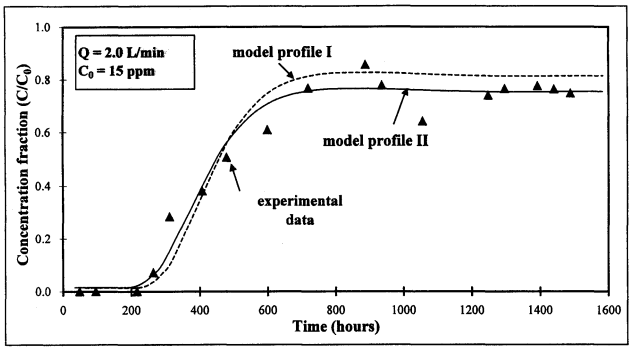

Figure 8. Experimental data and model profiles I and II for TCE in BF-3.

Model profile I: simulation based on the biokinetic parameters for microbial culture I; Model profile II: best-fit simulation.

bers, are defined as follows

$$Sh = \frac{d_p k_f}{D_w}; \quad Re_p = \frac{d_p V_x \rho_g}{\mu_g}; \quad Sc = \frac{\mu_g}{\rho_g D_w} \tag{39}$$

The number of particles within a defined bed layer was estimated using the following equations

N_{total} = number of particle in the packing volume

$$= \frac{\text{Mass (total volume)}}{\text{Mass (single particle)}}$$

$$= \frac{V_{\text{total}} \times \rho_b}{V_p \times \rho_s} = \frac{V_{\text{total}} \times (1-\epsilon)\rho_s}{V_p \times \rho_s} = \frac{V_{\text{total}} \times (1-\epsilon)}{V_p} \tag{40}$$

where V_p and V_{total} represent the volume of a single particle and the total packed volume, respectively; ρ_s is the particle density, and ρ_b is the particle bulk density.

Defining that the elemental bed layer thickness is equivalent to the mean particle diameter, then the number of bed layers and the number of particles in each layer can be easily obtained

$$Z = \text{number of layers in the column} = \frac{L}{2R_1} \tag{41}$$

$$N = \text{number of particles per layer} = \frac{N_{\text{total}}}{Z} \tag{42}$$

The values of all mass transfer parameters are summarized in Table 2.

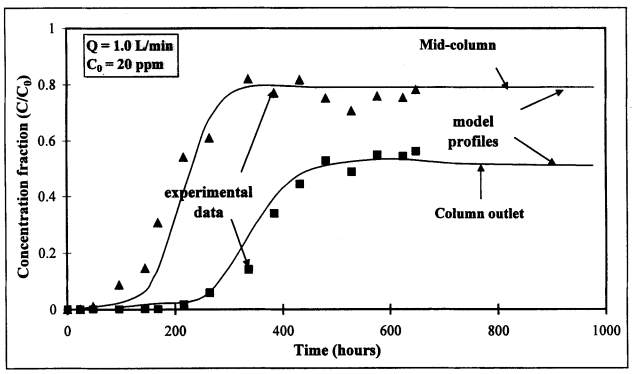

Figure 7. Experimental data and model profiles for TCE in BF-2 at mid-column and column outlet positions.

Bench-scale biofilter studies

Bench-scale biofilter column studies were conducted to evaluate the removal efficiencies for the organic contaminant of interest, and to validate the model. These columns were subjected to different operating conditions as specified in Table 1. The input parameters used for model simulations, as well as the pre-determined operating conditions, are listed in Table 2.

The experimental breakthrough data and model profiles at two specific positions (mid-column and outlet) for columns BF-1 and BF-2 are presented in Figures 6 and 7, respectively. In both cases, a good agreement was observed between the experimental data and the predicted model profiles. Figure 8 shows the experimental data and predicted profiles for column BF-3, which was inoculated with a different mixture of microbial culture and for which biokinetic parameters were not determined (Table 1). For comparison purposes, two effluent concentration profiles predicted by the model are presented, wherein the dotted line (model profile I) shows the simulation corresponding to biokinetic parameters obtained for mixed culture I, and the solid line (model profile II) denotes best-fit simulation. The differences between the two simulation profiles (Figure 8) illustrate that the biodegradation potential of microbial culture I is significantly lower than that of microbial culture II. It is evident that both profiles are in good agreement with the experimental data.

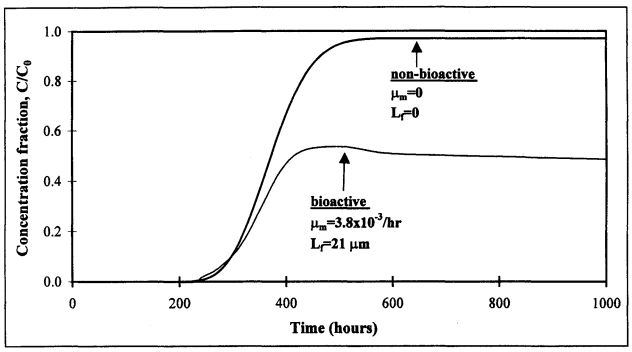

Figure 9. Simulated concentration breakthrough profiles: bioactive vs. nonbioactive models.

Dynamic simulations

Model simulation studies were conducted under various conditions to examine the dynamic behavior of the model, and model sensitivity studies to examine the variations in biofilter dynamics with reference to selected parameters. The model parameters used in these dynamic simulations and sensitivity analyses are categorically listed in Table 2.

Simulation results for the bioactive (adsorption plus biofilm degradation) and nonbioactive (adsorption only) biofilter effluent concentration profiles are shown in Figure 9. It should be noted that the nonbioactive profile was simulated by suppressing biofilm thickness and neglecting biological, as well as mass-transfer parameters. Evidently, biofilm degradation greatly enhances the performance and useful life of GAC biofilters. Carbon adsorption is operative predominantly at the transient stage of the biofiltration process; however, biofilm degradation eventually displaces adsorption as the primary removal mechanism when the bioactive profile gradually levels off and reaches steady state. In contrast, the nonbioactive profile exhibits a complete breakthrough phenomenon similar to that experienced in a typical packed-bed adsorber. The simulations presented in Figure 10 further demonstrate the advantages underlying the combined effects of biodegradation and carbon adsorption over a range of EBCTs (2–8 min). In this investigation, the biofilter volume was so designed that desirable EBCTs could be obtained at the employed flow rates. The profiles clearly indicate that the favorable effects of bioactive GAC become more significant at longer EBCTs. Under these conditions, biodegradation not only lengthens the breakthrough times, but also achieves improved steady-state contaminant removals.

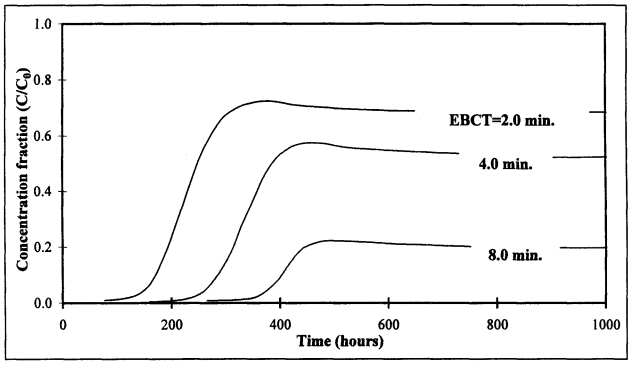

Figure 10. Model simulation profiles for biofilter performance at different EBCTs.

The effect of mass-transfer barrier due to the external aqueous film on the process dynamics is represented in Figure 11. The aqueous film is attributed to the intermittent supply of nutrient solution to the biofilter medium, and is assumed to form a stagnant layer surrounding the biofilm for the purpose of demonstrating its influence. Any loss of water would thus be immediately replenished by an external supply. Under this condition, the steady-state removal efficiency (solid line) for a water film of thickness 20 μm is approximately reduced by 5% in comparison to that for a film thickness of 5 μm, as shown in Figure 11. Further increase in film thickness would lead to greater reduction in steady-state removal efficiency. The effects of the water content has also been discussed by Wang and Govind (1997) in their model for biofilters using peat and compost for the treatment of isopentane vapor. Although their discussion was based on intraparticle transport and biodegradation, they suggested the existence of an optimum water content, above which the biofilter performance would decline due to increased mass-transfer resistance. The effects of aqueous film demonstrates the engineering significance of maintaining appropriate moisture content in biofilter media, particularly if the target volatile organic compounds are characterized by high values of Henry's Law constants (low water solubility) and low values of liquid diffusivities.

Bioregeneration phenomenon

Bioregeneration is a term commonly used to describe the application of biodegradation for recovering the adsorptive capacity of GAC (Speitel et al., 1987; Kim and Pirbazari, 1989). In order to investigate the effects of bioregeneration in biofilters, a surface contour showing the time-dependent effluent concentration profile with respect to the radial position within an activated carbon particle was simulated in Figure 12. The TCE concentrations in the biofilm (aqueous phase) and particle (solid phase) were normalized independently according to the nondimensionalization procedure described earlier (that is, $\bar{s}_f = s_f/s_0$; $\bar{q} = q/q_0$). It can be observed that, during the initial operating period, a steady mass flux of TCE was being transported inward (indicated by the arrow direction) into the particle due to diffusional adsorption and mass transport. As the system gradually becomes bioactive, the aqueous substrate concentration at the vicinity of the biofilm/particle interface would gradually become lower than that of the solid concentration, causing the substrate to diffuse out of the carbon for biofilm degradation. This desorption phenomenon re-opens the adsorption sites on the carbon particle to more contaminant uptake. Eventually, a flux balance between the substrate concentrations in the aqueous and solid phases is attained as the process approaches equilibrium.

Bioregeneration mechanism represents several distinct advantages in biofilter applications. It is widely accepted that it can enhance biodegradation of slowly or poorly biodegradable compounds by retention on carbon surfaces (Schultz and

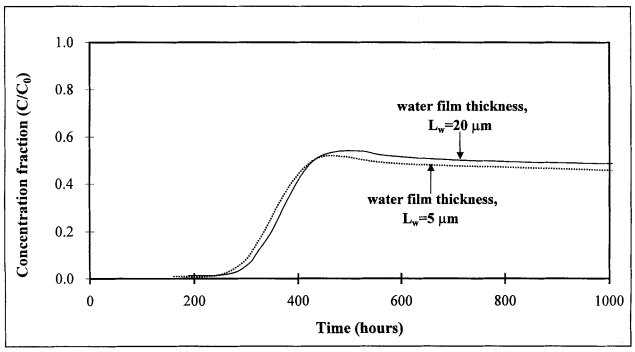

Figure 11. Simulated performance profiles for hypothetically up-scaled biofilters.

Keinath, 1984), and, additionally, can dampen the adverse effects of concentration fluctuations in waste gas streams (Ying and Weber, 1979). Furthermore, in the treatment of recalcitrant compounds such as TCE bioregeneration offers protection of microorganisms from toxic inhibition arising from intermediate products. Several investigators have shown that intermediate metabolites of TCE can be deleterious to microorganisms, causing deterioration of cell viability (Wackett and Gibson, 1988; Oldenhuis et al., 1991; Bielefeldt et al., 1995). With bioregeneration, these toxic intermediates can be effectively adsorbed onto carbon surfaces, so that their inhibitory effects on microorganisms can be alleviated.

Scale-up simulation studies

Scale-up simulation studies were conducted to obtain an engineering appreciation for industrial-scale biofilter design and operation for meeting the hypothetical TCE treatment objectives. These investigations also illustrate the utility of modeling and upscaling techniques employed to obtain *a priori* evaluation of biofilter performance with minimal time and effort in pilot testing. Furthermore, they demonstrate the usefulness of a modular design approach for meeting treatment objectives under certain site-specific constraints.

The results of industrial-scale biofilter simulations are depicted in Figure 13. As shown in Table 3, the equivalent volume of the biofilter was varied to obtain assessments of their treatment efficiencies for a waste stream with an emission flow rate of 2 m^3/min and TCE concentration of 100 mg/m^3. The performance prediction was evaluated by using a series of biofilter modules, each being 2.0 m in depth and 1.5 m in diameter. As evident from Figure 13, when the number of modules was increased from 1 to 2 (corresponding to profiles

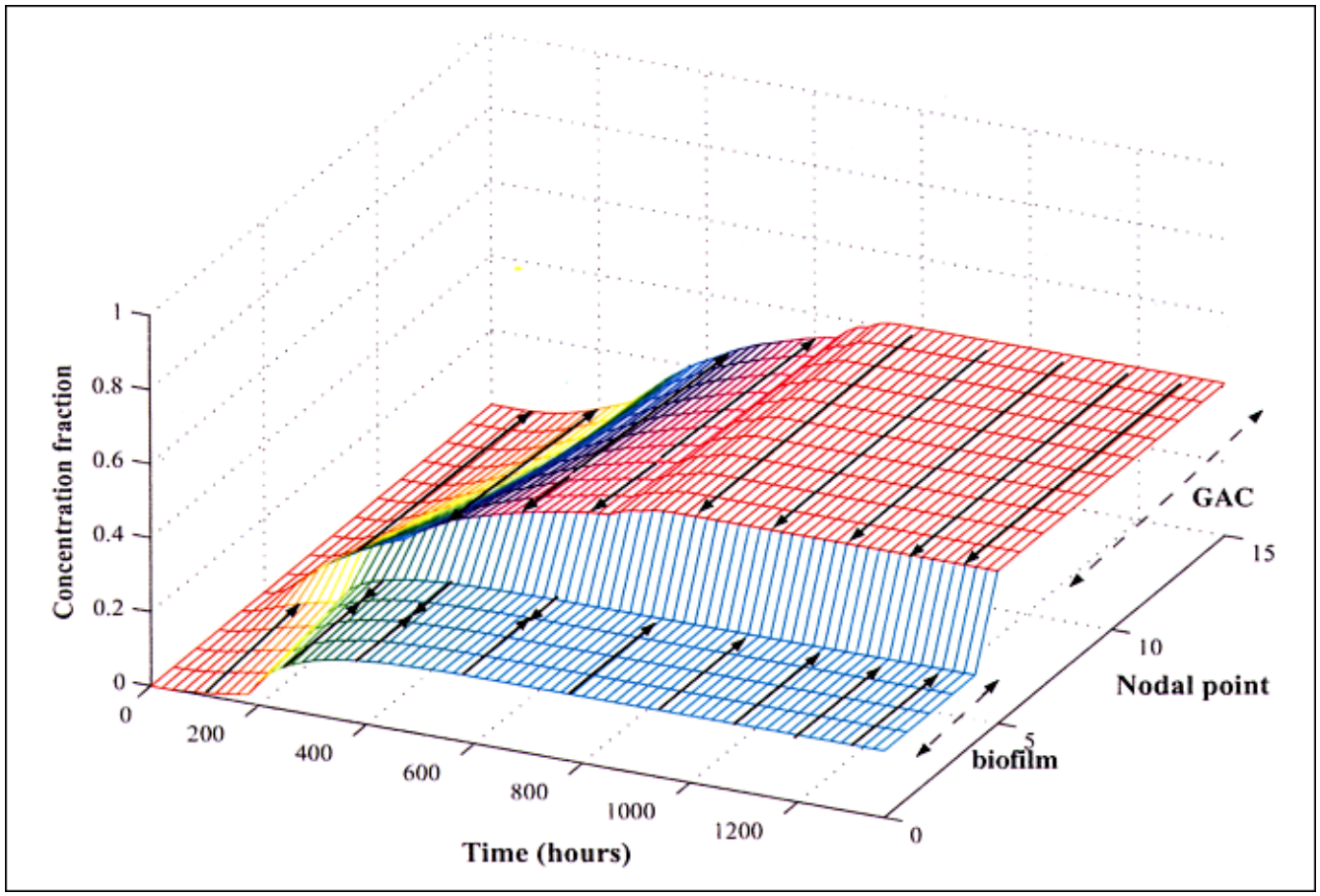

Figure 12. Model simulation showing the concentration profiles along the biofilm/particle radius and bioregeneration effects.

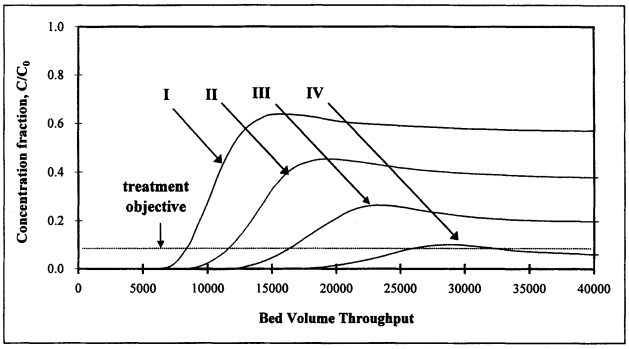

Figure 13. Performance predictions for industrial-scale biofilter using different reactor lengths.

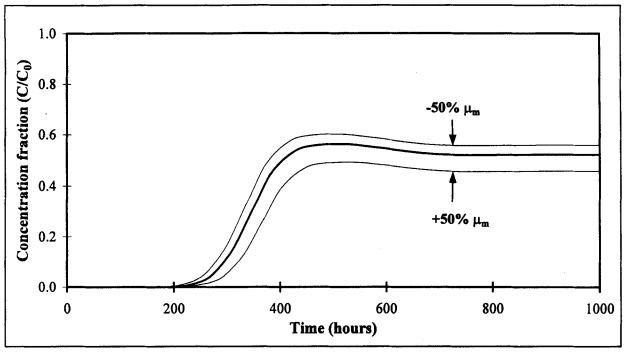

Figure 14. Model sensitivity analysis for maximum substrate utilization rate, μ_m.

I and II, respectively), the predicted steady-state removal efficiency correspondingly improved from 43.6% to 62.3%; and an additional module (profile III) further enhanced the efficiency to about 80%. However, if the treatment efficiency were assumed to be 90%, then at least five modules would be required (profile IV). In summation, these studies demonstrate the usefulness of flexibility in reactor design most suitable for site-specific installations. For example, if a roof-top installation has a height limitation and requires uniform weight distribution, then a biofilter can be designed with multiple modules of identical dimensions operating in series (as depicted in Table 3). Furthermore, this modular design approach accommodates alternate (backup) units for temporary shutdown and maintenance operations.

Sensitivity analyses and engineering implications

Sensitivity analyses were conducted with two specific objectives: to study the effects of various parameters on biofilter performance, and to determine what conditions must be altered to improve it. The parameters that were varied to evaluate their effects on the model effluent profiles included the following: Monod constants (μ_m and K_s), the biofilm thickness (L_f), the Freundlich isotherm constant (K_F and n), and mass-transfer parameters (k_f, D_f, D_g, and D_w). A deviation of 50% on both upper and lower bounds of the standard conditions (Table 2) for each parameter was tested.

The results of sensitivity studies for the biokinetic parameters, μ_m and K_s, are shown in Figures 14 and 15, respectively. As evident from Figure 14, the effluent concentration profiles were significantly influenced by the maximum substrate utilization rate μ_m. Under these conditions, the maximum substrate utilization rate was more influential than the half-saturation constant. For example, an increase of 50% in μ_m yielded improvement in biofilter performance by more than 15% under steady-state conditions. A decrease of 50% in K_s, however, led to less than 10% improvement in the steady-state performance.

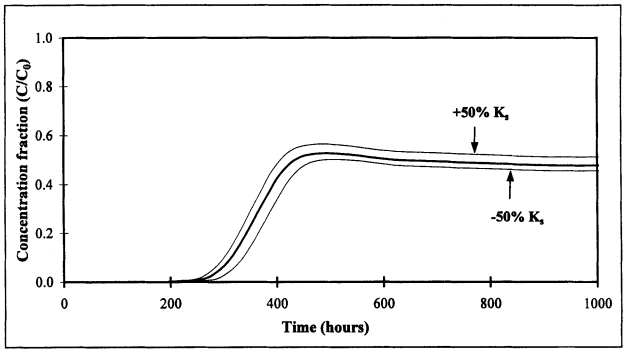

Figure 15. Model sensitivity analysis for half-saturation constant K_s.

Figure 16 shows the effects of variations in biofilm thickness L_f, a parameter that generally has a profound influence on the steady-state removal efficiency of the biofilter. Some

Table 3. Biofilter Characteristics for Scale-Up Simulation Studies

Model Profile	No. of Biofilter Modules	Total Bed Depth (cm)	EBCT (min)	Pred. Steady-State Removal Eff. (%)
I	1	200	1.8	43.6
II	2	400	3.6	62.5
III	3	600	5.4	80.5
IV	5	1,000	9.0	94.7

Common parameters: Depth of biofilter module = 2 m; column diameter = 1.5 m; gas flow rate = 2.0 m^3/min; influent TCE concentration = 100 mg/m^3; particle diameter = 4.0 mm.

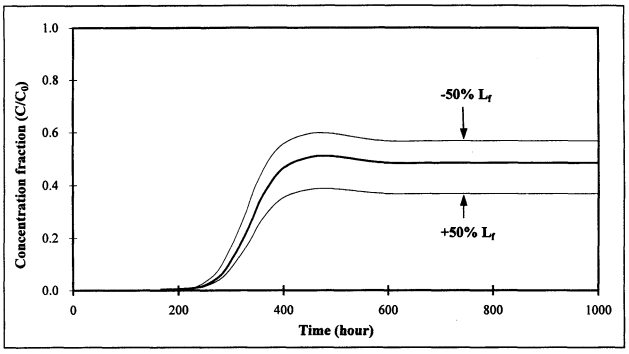

Figure 16. Model sensitivity analysis for biofilm thickness L_f.

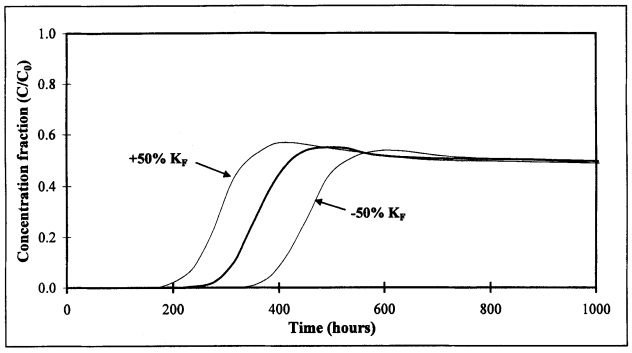

Figure 17. Model sensitivity analysis for Freundlich isotherm capacity constant K_F.

interesting trends were observed in these simulations. A 50% increase in biofilm thickness resulted in a substantial improvement of about 20% in the steady-state performance, increasing the intrinsic contaminant removal from 50% to 60%. On the other hand, a 50% decrease in the parameter led to a reduction in contaminant removal from 50% to 45%. In the present situation, an increase in biofilm thickness resulted in an improved performance of the biofilter due to higher biomass. Nonetheless, increasing the biofilm thickness could sometimes lower the process efficiency. It must be noted that the biofilm thickness and density are widely regarded as the most critical parameters for efficient operation of biofilm reactors. Increase in cell density or biofilm thickness increases both the reaction rate and the mass-transfer resistance. Therefore, for a given type and concentration of a growth substrate, an optimum balance must be realized between biofilm density and thickness to maximize the pollutant consumption rate.

The effects of variations in the adsorption equilibrium parameters, K_F and n, are shown in Figures 17 and 18, respectively. A 50% increase in the Freundlich capacity constant K_F manifested a delay in the column breakthrough from 450 h to 600 h before becoming predominant biodegradation, while a 50% decrease in the parameter showed advancement in breakthrough to 400 h. However, the steady-state dynamics of the biofilter were not affected by variations in K_F. Qualitatively similar results were observed for variations in the adsorption intensity constant n. A 50% increase in n reflected the occurrence of an earlier breakthrough; whereas, a

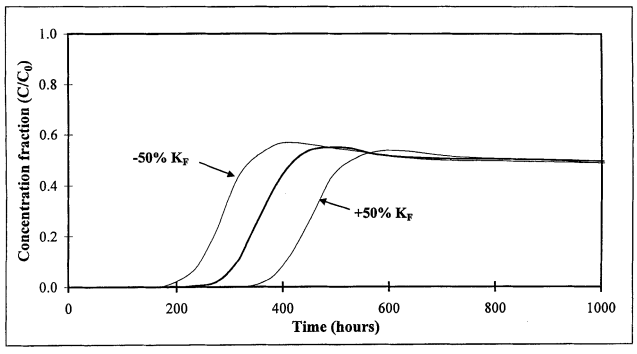

Figure 18. Model sensitivity analysis for the Freundlich isotherm constant n.

50% decrease in the parameter exhibited a slower breakthrough and increased utilization of adsorbent capacity. Nonetheless, the steady-state biofilter effluent profiles remained unaffected due to changes in n. Evidently, the variation in the Freundlich equilibrium parameters significantly influenced the breakthrough profiles at the earlier stages of biofilter operation; however, practically no effect was observed in the steady-state region. These results suggest that the TCE removal was markedly influenced by adsorption equilibrium only during the transient phase of biofilter operation.

Sensitivity analyses were also performed for several mass-transfer parameters including the following: the film transfer coefficient (k_f), biofilm diffusion coefficient (D_f), gas diffusion coefficient (D_g), and free liquid aqueous phase diffusivity (D_w). These studies clearly indicated that the effects of these mass-transfer parameters on the process dynamics were marginal, implying that the biofilter operation regime was not mass-transfer rate-limiting under the process conditions assumed for TCE removal.

Model sensitivity studies demonstrated that the biological parameters pertaining to biokinetic constants and biofilm properties were important factors for consideration in order to achieve better removal efficiencies. In principle, enhancement of these parameters can be accomplished from microbial strain and enzyme activity improvement, as well as biofilm maintenance. The utility of microbial strain improvement arises due to the recalcitrance of a substrate that serves as both electron donor and primary energy source under aerobic conditions. However, successes experienced in the field of industrial microbiology strongly suggest that strain improvement through nonrecombinant (that is, induced mutagenesis, protoplast fusion, and plasmid conjugation) and recombinant (that is, genetically engineered) techniques can significantly accelerate metabolic rates of target contaminants (Vinci and Byng, 1999). Furthermore, enhanced enzyme activity by sequential application of several enzymes would not only increase the maximum substrate utilization rate (μ_m), but also reduce the half-saturation constant (K_s) (Atlas and Unterman, 1999).

Summary and Conclusions

The major findings of this study may be briefly summarized as follows:

- A systematic protocol was developed using a mathematical modeling technique and an experimental approach. Trichloroethylene, a chlorinated VOC of major environmental concern, was employed as the test pollutant. The biological and adsorption parameters were independently determined from carefully designed laboratory-scale experiments. Good agreements between the experimental breakthrough data and model predictions were observed under different operating conditions, validating the biofiltration model.
- Simulation studies comparing the "bioactive" and "nonbioactive" scenarios revealed that the complementary removal mechanisms of biodegradation and adsorption greatly enhance the overall treatment efficiency. The effects of bioregeneration phenomenon in GAC biofilters were demonstrated, highlighting that adsorption was an important re-

moval mechanism during the transient phase of biofilter operation.

• Scale-up considerations and methods were developed based on dimensional analysis and similitude. For practical design considerations, the scale-up techniques provides an effective tool for *a priori* evaluation of biofilter performance, and substantially reduces the costs associated with pilot-scale and full-scale testing.

• Sensitivity analysis indicated that the Monod constants (μ_m and K_s), as well as the biofilm thickness (L_f), significantly influenced the biofilter performance. Variations in the Freundlich isotherm constants (K_F and n) markedly influenced the column breakthrough profile, but only marginally affected the steady-state performance. These sensitivity analyses may provide insight with regard to potential biofilter performance improvement. Furthermore, it was found that the mass-transfer barrier caused by the liquid film adversely influenced the steady-state TCE removal.

Acknowledgments

Part of this research was presented at the AIChE Annual Meeting in Los Angeles, Nov. 12–17, 2000.

Financial support for this research was partially provided by the National Nano Device Laboratory of the Republic of China. The authors are grateful to Varadarajan Ravindran and Shih-Chieh Tu for their diligent technical assistance in this research.

Notation

A_p = surface area of a particle, L^2
c = substrate concentration in gas film, M/L^3
c_b = substrate concentration in bulk gas, M/L^3
C_e = effluent gas-phase concentration, M/L^3
C_0 = influent gas-phase concentration, M/L^3
D_g, D_w, D_f, and D_s = substrate diffusion coefficient in gas phase, aqueous phase, biofilm, solid phase, respectively, L^2/T
$D_{g,s}$ = surface solute distribution parameter, dimensionless
Da_{ft}, Da_s, Da_{ov} = Damköhler number with respect to film transfer, surface diffusion, and overall process, respectively, dimensionless
E_r = biochemical reactivity modulus, dimensionless
E_s = surface diffusivity modulus, dimensionless
H_c = Henry's Law constant, dimensionless
k = biochemical reaction parameter, $1/T$
k_f = film transfer rate coefficient, L/T
K_F = adsorption capacity constant for Freundlich isotherm, $M/M\ L^3/M^n$
K_s = half-saturation constant for Monod kinetics, M/L^3
L = packed bed length, L
L_f = biofilm thickness, L
L_w = water film thickness, L
M = substrate mass adsorbed in a particle, M
$M_{\text{in},i}$ = substrate mass entering an incremental layer, M
$\Delta M_{\text{total},i}$ = substrate mass removed within an incremental layer, M
N_p = number of particles, dimensionless
n = adsorption intensity constant for Freundlich isotherm, dimensionless
Pe, Pe_p = column and particle Peclet numbers, dimensionless
q = solid-phase substrate concentration in adsorbent particle, M/M
q_s = solid-phase substrate concentration at particle surface, M/M
r = radial coordinate, L
R_1, R_2, R_3, and R_4 = radius of particle, particle + biofilm, particle + biofilm + water film, and particle + biofilm + water film + gas film, respectively, L
Re_p = particle Reynolds number, dimensionless
s^* = substrate concentration at gas/water interface, M/L^3
s_f = aqueous phase substrate concentration in biofilm, M/L^3
$s_{f,s}$ = substrate concentration at biofilm/solid interface, M/L^3
s_w = aqueous phase substrate concentration in water film, M/L^3
$s_{w,f}$ = substrate concentration at water/biofilm interface, M/L^3
Sh = Sherwood number, dimensionless
Sc = Schmidt number, dimensionless
St = Stanton number, dimensionless
t = time scale, T
V_p = volume of particle, L^3
V_L = volume of defined bed layer, L^3
V_x = gas flow velocity, L/T
v_g = gas-flow velocity, L/T
X_f = biofilm density, M/L^3
Y = microbial yield coefficient, M/M
ΔW_1 = weight of evaporated water, M
ΔW_2 = dry cell weight, M
α, β = weighted factors for scale-up relation
$\alpha_g, \alpha_w, \alpha_f, \alpha_s$ = dimensionless groups for substrate diffusivity in gas, aqueous, biofilm, and solid phase, respectively
ϵ = packed-bed porosity, dimensionless
μ_g = gas viscosity, $M/(L \cdot T)$
μ_m = maximum substrate utilization rate constant for Monod kinetics, $1/T$
ρ_b = bulk density of media particles, M/L^3
ρ_g = gas density M/L^3
ρ_l = aqueous density, M/L^3
ρ_s = particle density, M/L^3
θ = mean residence time for minibiofilter, T
ω_1, ω_2 = dimensionless groups for Monod kinetic constants
$\phi_1, \phi_2, \gamma, \delta$ = dimensionless groups for boundary conditions
τ_c = breakthrough time, T

Literature Cited

Abu-Reesh, I. M., "Predicting the Performance of Immobilized Enzyme Reactors Using Reversible Michaelis-Menten Kinetics," *Bioproc. Eng.*, **17**, 131 (1997).

Atlas, R. M., and R. Unterman, "Bioremediation," *Manual of Industrial Microbiology and Biotechnology*, 2nd ed., A. L. Damain, et al., eds., ASM Press, Herdon, VA, p. 666 (1999).

Bartha, R., and D. Pramer, "Features of a Flask and Method for Measuring the Persistent and Biological Effects of Pesticides in Soil," *Soil Sci.*, **100**, 68 (1965).

Bielefeldt, A. R., H. D. Stensel, and S. E. Strand, "Cometabolic Degradation of TCE and DCE without Intermediate Toxicity," *J. Environ. Eng.*, **121**, 791 (1995).

Clean Air Act Amendments of 1990, Public Law, 101–549, 104 Stat. 2399 (Nov. 15, 1990).

Crittenden, J. C., and W. J. Weber, Jr., "Predictive Model for Design of Fixed-Bed Adsorbers: Parameter Estimation and Model Development," *Environ. Eng. Div. (ASCE)*, 104 (EE2), 185–197 (1978a).

Crittenden, J. C., and W. J. Weber, Jr., "Predictive Model for Design of Fixed-Bed Adsorbers: Single Component Model Verification," *Environ. Eng. Div. (ASCE)*, 104 (EE3), 433–443 (1978b).

Crittenden, J. C., and D. W. Hand, "Design of Rapid Small-Scale Adsorption Tests for a Constant Diffusivity," *J. Wat. Pollut. Contr. Fed.*, **58**, 312 (1986).

Crittenden, J. C., J. K. Berrigan, D. W. Hand, and B. Lykins, "Design of Rapid Fixed-Bed Adsorption Tests for Nonconstant Diffusivity," *J. Environ. Eng.*, **113**, 243 (1987).

Crittenden, J. C., P. S. Reddy, H. Arora, J. Trynoski, D. W. Hand, D. L. Perram, and R. S. Summers, "Predicting GAC Performance with Rapid Small-Scale Test Columns," *J. Am. Wat. Works Assoc.*, **83**, 1153 (1991).

De heyder, B., A. Overmeire, H. van Langenhove, and W. Verstraete, "Ethene Removal from a Synthetic Waste Gas Using a Dry Biobed, "*Biotechnol. Bioeng.*, **44**, 642 (1994).

Deshusses, M. A., G. Hamer, and I. J. Dunn, "Behavior of Biofilters for Waste Air Biotreatment. 1. Dynamic Model Development," *Environ. Sci. Technol.*, **29**, 1048 (1995).

Diks, R. M. M., and S. P. P. Ottengraf, "Verification Studies of a Simplified Model for the Removal of Dichloromethane from Waste Gases Using a Biological Trickling Filter (Part I)," *Bioproc. Eng.*, **6**, 93 (1991).

Dwivedi, P. N., and S. N. Upadhyay, "Particle-Fluid Transfer in Fixed and Fluidized Beds," *Ind. Eng. Chem. Proc. Des. Dev.*, **16**, 157 (1977).

Fan, L.-S., R. Leyva-Ramos, K. D. Wisecarver, and B. J. Zehner, "Diffusion of Phenol Through a Biofilm Grown on Activated Carbon Particles in a Draft-Tube Three-Phase Fluidized-Bed Bioreactor," *Biotechnol. Bioeng.*, **35**, 279 (1990).

Fuller, E. N., P. D. Schettler, and J. C. Giddings, "A New Method for Prediction of Binary Gas-Phase Diffusion Coefficients," *Ind. Eng. Chem.*, **58**, 18 (1966).

Hyduk, W., and H. Laudie, "Prediction of Diffusion Coefficients in Nonelectrolytes in Dilute Aqueous Solutions," *AIChE J.*, **20**, 611 (1974).

Hayduk, W., and B. S. Minhas, "Correlation for Prediction of Molecular Diffusivities in Liquids," *Can. J. Chem. Eng.*, **60**, 295 (1982); Correction, **61**, 132 (1983).

Hodge, D. S., and J. S. Devinny, "Modeling Removal of Air Contaminants by Biofilter," *J. Environ. Eng.*, **121**, 21 (1995).

Kim, S.-H., and M. Pirbazari, "Bioactive Adsorber Model for Industrial Wastewater Treatment," *J. Environ. Eng.*, **115**, 1235 (1989).

Kleijn, C. R., K. J. Kuijlaars, and H. E. A. Van der Akker, "Design and Scale-up of Chemical Vapor Deposition Reactors for Semiconductor Processing," *Chem. Eng. Sci.*, **51**, 2119 (1995).

Law, A. T., B. R. Robertson, S. S. Dunker, and D. K. Button, "On Describing Microbial Growth Kinetics from Continuous Culture Data: Some General Considerations, Observations, and Concepts," *Microbial Ecology*, **2**, 261 (1976).

Man, M. K., B. N. Badriyha, W. Den, and M. Pirbazari, "Vapor Phase Biofiltration for Removal of VOCs," *Proc. of 1996 North American Water Environment Congress*, ASCE, Anaheim, CA (1996).

McKelvey, J. M., and H. E. Holescher, "Apparatus for Preparation of Very Dilute Gas Mixture," *Anal. Chem.*, **29**, 123 (1957).

Miller, R. E., and F. P. Guengerich, "Metabolism of Trichloroethylene in Isolated Hepatocytes, Microsomes, and Reconstituted Enzyme Systems Containing Cytochrome P-450," *Cancer Res.*, **43**, 1145 (1983).

Oldenhuis, R., J. Y. Oedzes, J. J. V. D. Waarde, and D. B. Janssen, "Kinetics of Chlorinated Hydrocarbon Degradation by *Methylosinus trichosporium* OB3b and Toxicity of Trichloroethylene," *Appl. Environ. Microbiol.*, **57**, 7 (1991).

Pirbazari, M., B. N. Badriyha, and R. J. Miltner, "GAC Adsorber Design for Removal of Chlorinated Pesticides," *J. Environ. Eng.*, **107**, 80 (1991).

Pirbazari, M., V. Ravindran, B. N. Badriyha, S. Craig, and M. J. McGuire, "GAC Adsorber Design Protocol for the Removal of Off-Flavors," *Wat. Res.*, **27**, 1153 (1993).

Ravindran, V., M. R. Stevens, B. N. Badriyha, and M. Pirbazari, "Modeling the Sorption of Toxic Metals on Chelant-Impregnated Adsorbent," *AIChE J.*, **45**, 1135 (1999).

Ravindran, V., S. H. Kim, B. N. Badriyha, and M. Pirbazari, "Predictive Modeling for Bioactive Fluidized Bed and Stationary Bed Reactors: Application to Dairy Wastewater," *Environ. Technol.*, **18**, 861 (1997).

Schultz, J. R., and T. M. Keinath, "Powder Activated Carbon Treatment Process Mechanisms," *J. Wat. Pollut. Contr. Fed.*, **56**, 143 (1984).

Shareefdeen, Z., and B. C. Baltzis, "Biofiltration of Toluene Vapor Under Steady-State and Transient Conditions: Theory and Experimental Results," *Chem. Eng. Sci.*, **49**, 4347 (1994).

Siddiqi, M. A., and K. Lucas, "Correlations for Prediction of Diffusion in Liquids," *Can. J. Chem. Eng.*, **64**, 839 (1986).

Speitel, G. E., Jr., K. Dovantzis, and F. A. DiGiano, "Mathematical Modeling of Bioregeneration in GAC Columns," *J. Environ. Eng.*, **113**, 32 (1987).

Speitel, G. E., Jr., and D. S. McLay, "Biofilm Reactors for Treatment of Gas Streams Containing Chlorinated Solvents," *J. Environ. Eng.*, **119**, 658 (1993).

Sun, A. K., J. Hong, and T. K. Wood, "Modeling Trichloroethylene Degradation by a Recombinant Pseudomonad Expressing Toluene *ortho*-Monoxygenase in a Fixed-Film Bioreactor," *Biotechnol. Bioeng.*, **59**, 40 (1998).

Tang, W.-T., and L.-S. Fan, "Steady State Phenol Degradation in a Draft-Tube, Gas-Liquid-Solid Fluidized-Bed Bioreactor," *AIChE J.*, **33**, 239 (1987).

Tang, H.-M., S.-J. Hwang, and S.-C. Hwang, "Waste Gas Treatment in Biofilters," *J. Air & Waste Manage. Assoc.*, **46**, 349 (1996).

Taylor, R., and R. Krishna, *Multicomponent Mass Transfer*, Wiley, New York (1993).

Vinci, V. A., and G. Byng, "Strain Improvement by Nonrecombinant Methods," *Manual of Industrial Microbiology and Biotechnology*, 2nd ed., A. L. Damain, et al., eds., ASM Press, Herdon, VA 103 (1999).

Wackett, L. P., and D. T. Gibson, "Degradation of Trichloroethylene by Toluene Dioxygenase in Whole-Cell Studies with Pseudomonas Putida F1," *Appl. Environ. Microbiol.*, **54**, 1703 (1988).

Wang, Z., and R. Govind, "Biofiltration of Isopentane in Peat and Compost Packed Beds," *AIChE J.*, **43**, 1348 (1997).

Wilke, C. R., and P. Chang, "Correlation of Diffusion Coefficients in Dilute Solutions," *AIChE J.*, **1**, 264 (1955).

Ying, W., and W. J. Weber, Jr., "Bio-Physicochemical Adsorption Model Systems for Wastewater Treatment," *J. Wat. Pollut. Contr. Fed.*, **51**, 2661 (1979).

Zauner, R., and A. G. Jones, "Scale-up of Continuous and Semi-batch Precipitation Processes," *Ind. Eng. Chem. Res.*, **39**, 2392 (2000).

Zerook, S. M., A. A. Shaikh, and Z. Anzar, "Development, Experimental Validation and Dynamic Analysis of a General Transient Biofilter Model," *Chem. Eng. Sci.*, **52**, 759 (1997).

Manuscript received Jan. 17, 2001, and revision received Mar. 15, 2002.